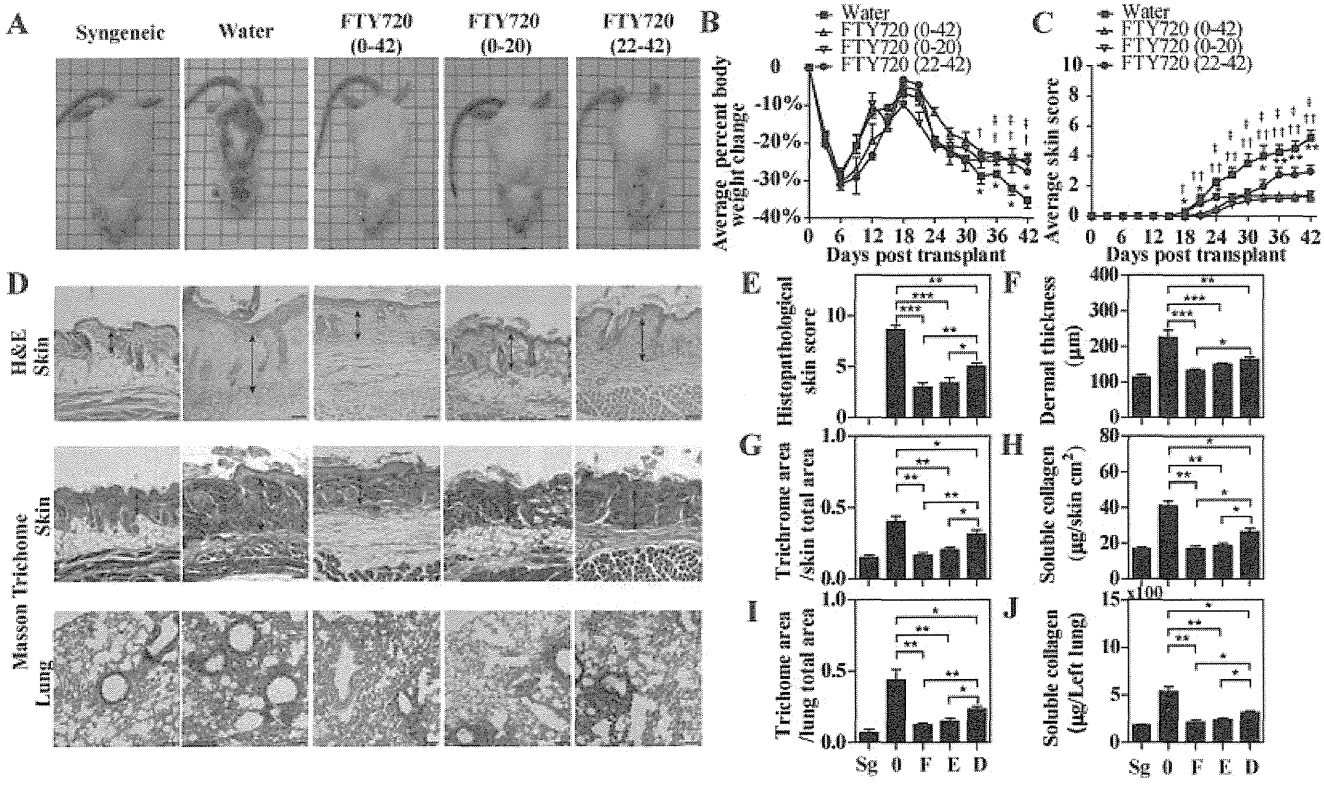

Figure 1. Oral early treatment with FTY720 inhibits and delayed treatment with FTY720 attenuates the severity and fibrosis of murine sclerodermatous chronic graft-versus-host disease. Recipients were given sterile water or were orally administered FTY720 (1 mg/kg/day) from day 0 to day 42 (full-term, early-treatment group), from day 0 to day 20 (short-term, early-treatment group), or from day 22 to day 42 (delayed-treatment group). A control syngeneic group of female BALB/c mice received male BALB/c mouse T cell–depleted bone marrow (BM) cells and splenocytes (syngeneic BM transplantation [BMT]). **A,** Representative photographs were taken 42 days after BMT. **B** and **C,** Average body weight changes (**B**) and skin scores (see Materials and Methods for details) (**C**) were monitored every 3 days from day 0 to day 42. Values are the mean ± SEM of 4–6 mice per group. * = $P < 0.05$; ** = $P < 0.01$ for full-term, early-treatment group or short-term, early-treatment group versus delayed-treatment group. † = $P < 0.05$; †† = $P < 0.01$ for full-term, early-treatment group or short-term, early-treatment group versus water-treated group. ‡ = $P < 0.05$ for delayed-treatment group versus water-treated group. **D,** Shown are representative photomicrographs of histopathologic changes in the 5 experimental groups. Tissue sections were stained with hematoxylin and eosin (H&E) or Masson's trichrome. **Arrows** indicate dermal thickness. Bars = 100 μm. **E,** Histopathologic skin scores were analyzed 42 days after BMT. **F–H,** Skin fibrosis was compared by determining dermal thickness (**F**), the ratio of trichrome-stained area to skin total area (**G**), and soluble collagen levels (**H**). **I** and **J,** Lung fibrosis was estimated by the ratio of trichrome-stained area to lung total area (**I**) and soluble collagen levels (**J**). Values are the mean ± SEM of 4–6 mice per group. * = $P < 0.05$; ** = $P < 0.01$; *** = $P < 0.001$. Sg = control syngeneic group; O = water-treated group, F = full-term, early-treatment group; E = short-term, early-treatment group; D = delayed-treatment group.

chronic GVHD with a lower average weight loss ($P < 0.05$) (Figure 1B) and decreased average skin score ($P < 0.01$) (Figure 1C). Notably, FTY720 was able to ameliorate body weight loss and decrease skin score when it was administered early in the course of disease with both full-term and short-term early treatment. When compared with the water-treated group, mice receiving delayed treatment with FTY720 showed a marked recovery in body weight ($P < 0.05$) (Figure 1B) and an attenuated skin score ($P < 0.05$) (Figure 1C).

The observed trends in skin disease were also verified by histopathology. In both early and delayed treatment, histopathologic scores, dermal thicknesses, and soluble skin collagen and fibrosis area in the skin and lung in FTY720-treated groups were significantly lower than those in the water-treated group ($P < 0.05$) (Figures 1E–J).

Restoration of PTEN expression and normalization of Smad3 phosphorylation status by FTY720. PTEN expression was decreased and Smad3 phosphorylation status was increased in murine sclerodermatous chronic GVHD. FTY720 treatment restored PTEN ex-

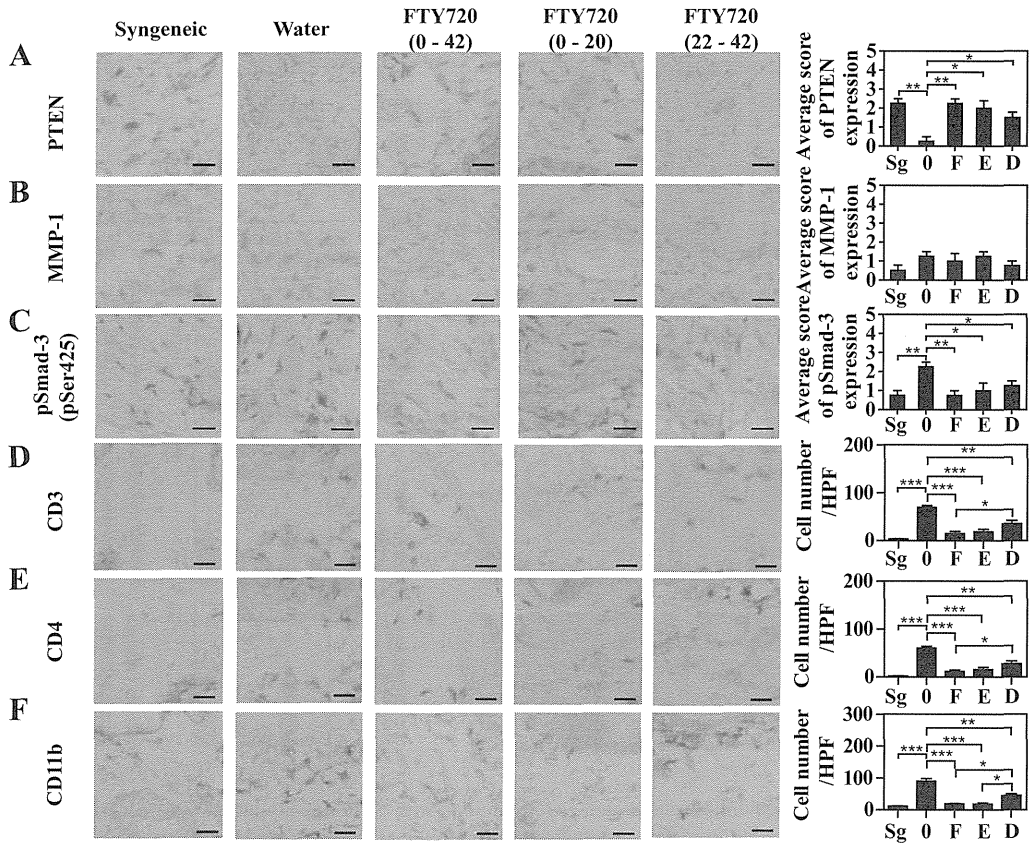

Figure 2. Restored phosphatase and tensin homolog (PTEN) expression, normalized Smad3 phosphorylation status, and decreased immune cell infiltration into skin in FTY720-treated animals. Immunohistochemical staining (left) was quantified (right). **A–C,** Skin tissues were harvested 42 days after BMT and assessed for expression of PTEN (**A**), matrix metalloproteinase 1 (MMP-1) (**B**), and Smad3 phosphoration (**C**) in spindle cells from groups of syngeneic mice, water-treated mice, and mice orally administered FTY720 from day 0 to day 42, from day 0 to day 20, and from day 22 to day 42 after BMT as described in Materials and Methods. **D–F,** Shown are numbers of CD3+ cells (**D**), CD4+ T cells (**E**), and CD11b+ cells (**F**) per high-power field (hpf) in the same treatment groups. Bars = 20 μm. Values are the mean ± SEM of 4–6 mice per group. * = $P < 0.05$; ** = $P < 0.01$; *** = $P < 0.001$. See Figure 1 for other definitions.

pression and normalized status of Smad3 phosphorylation (Figures 2A and C). However, the level of MMP-1 expression was not different in allogeneic groups as compared with syngeneic BMT in immunohistochemical staining slides (Figure 2B).

FTY720 treatment reduces the infiltration of CD4+ T cells and CD11b+ monocyte/macrophages into the skin. Immunohistochemical staining revealed that infiltration of CD3+ T cells, CD4+ T cells, and CD11b+ monocyte/macrophages into the skin was significantly inhibited in the FTY720-treated groups 42 days after BMT (Figures 2D–F). However, slides showed that very few B220+ B cells infiltrated into the skin (data not shown). The infiltration of CD3+ T cells, CD4+ T cells, and CD11b+ monocyte/macrophages was similar in the early-treatment groups; all were decreased in comparison to the delayed-treatment group.

FTY720 treatment decreases splenic CD4+ T cell numbers and increases splenic CD11b+Gr-1+ monocyte/macrophage numbers 7 days after BMT. The reaction of donor immune cells and recipient cells was inhibited by early treatment with FTY720. Seven days after BMT, the number of splenic CD4+ T cells was lower in syngeneic and FTY720-treated groups as compared with the water-treated group ($P = 0.041$ and $P = 0.047$, respectively) (Figure 3A). Splenic B220+ B cells and CD11b+ monocyte/macrophages were increased in allogeneic BM-transplanted mice; however, treatment with FTY720 significantly increased the numbers of B220+ B cells ($P = 0.037$) (Figure 3A) and CD11b+ monocyte/macrophages ($P = 0.04$) (Figure 3A). Nota-

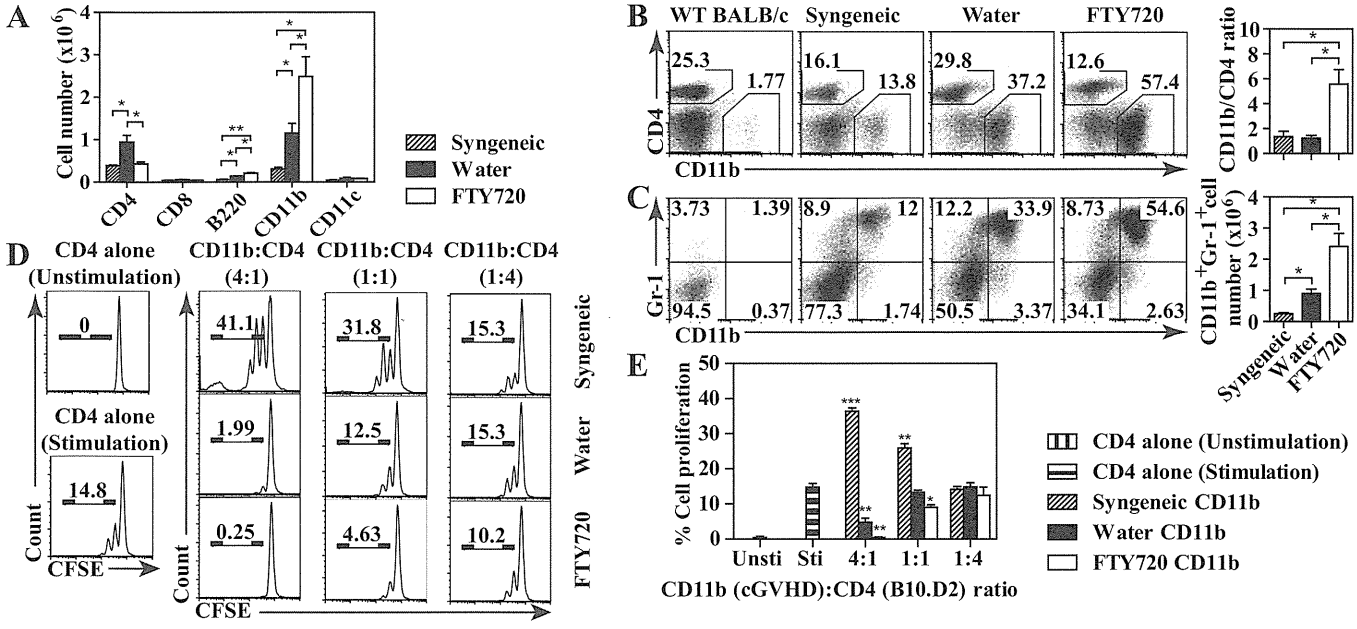

Figure 3. Early FTY720 treatment promotes invasion of myeloid-derived suppressor cells (CD11b+Gr-1+ cells), which inhibits CD4+ T cell proliferation. **A,** Shown are the numbers of splenic CD4+, CD8+, B220+, CD11b+, and CD11c+ cells 7 days after bone marrow transplantation (BMT). Values are the mean ± SEM of 4–5 mice per group. * = $P < 0.05$; ** = $P < 0.01$. **B,** Representative results demonstrate frequencies of splenic CD11b+ and CD4+ cells within the indicated gates among total live cells (left). Ratios of splenic CD11b+ to CD4+ cells 7 days after BMT are also shown (right). **C,** Representative results demonstrate frequencies of splenic CD11b+ and Gr-1+ cells within indicated gates among total live cells (left). Numbers of splenic CD11b+Gr-1+ cells 7 days after BMT are also shown (right). Values are the mean ± SEM of 4–5 mice per group. * = $P < 0.05$. **D,** Purified 5,6-carboxyfluorescein succinimidyl ester (CFSE)–labeled CD4+ T cells (4×10^5) were cocultured with various amounts of purified CD11b+ cells from syngeneic, FTY720-treated, and water-treated allogeneic BM-transplanted mice in the presence of plate-bound anti-CD3/anti-CD28 as described in Materials and Methods. After 48 hours, cells were harvested and analyzed by flow cytometry. **E,** Representative histograms show the proliferation of CD4+ T cells with different ratios of purified CD11b+Gr-1+ cells. Proliferation was measured by CFSE dilution. The experiment was performed in triplicate. Values are the mean ± SEM of 4–5 mice per group. * = $P < 0.05$; ** = $P < 0.01$; *** = $P < 0.001$ versus stimulated CD4+ T cells alone. WT BALB/c = wild-type BALB/c mice (without BMT); cGVHD = chronic graft-versus-host disease.

bly, FTY720 treatment significantly increased the ratio of CD11b+ cells to CD4+ cells 7 days post-BMT ($P = 0.03$) (Figure 3B) and resulted in an expansion in the number of splenic CD11b+Gr-1+ cells ($P = 0.029$) (Figure 3C).

The suppressive effects of allogeneic myeloid-derived suppressor cells (MDSCs; CD11b+Gr-1+ cells in mice) were demonstrated when splenic CD11b+ cells isolated from syngeneic, water-treated, and FTY720-treated mice 7 days post-BMT were cocultured with different ratios of CFSE-labeled B10.D2 mouse CD4+ T cells. Allogeneic, mouse-derived CD11b+ cells significantly inhibited CD4+ T cell proliferation, while syngeneic, mouse-derived CD11b+ cells activated CD4+ T cell proliferation when the ratio of CD11b to CD4 was 4:1 (Figures 3D and E).

FTY720 treatment induces increased Treg cell and Breg cell numbers via $S1P_1$ on day 14 after BMT. $S1P_1$ plays important roles in migration, development, and differentiation of T cells and B cells (29). After allogeneic BMT, splenic CD4+ T cells and CD19+ B cells increased $S1P_1$ expression when compared with syngeneic BMT. However, 14 days after BMT, FTY720 treatment markedly down-regulated the elevated expression of $S1P_1$ on CD4+ T cells (from a mean ± SEM of 26.00 ± 2.28% to 16.64 ± 1.72%; $P = 0.036$) and CD19+ B cells (from a mean ± SEM of 12.35 ± 1.18% to 6.51 ± 0.69%; $P = 0.03$) (Figure 4A).

The results indicated that regulatory cell subsets including CD4+CD25+ T cell and CD19+$CD1d^{high}$ CD5+ B cell populations showed significantly higher $S1P_1$ expression than CD4+CD25– T cell and CD19+ $CD1d^{intermediate}$CD5– B cell populations, respectively ($P < 0.001$) (Figure 4A). Additionally, FTY720 treatment reduced $S1P_1$ expression in CD4+CD25+ T cell and CD19+$CD1d^{high}$CD5+ B cell populations.

Fourteen days post-BMT, when compared with the water-treated group, the percentage and number of

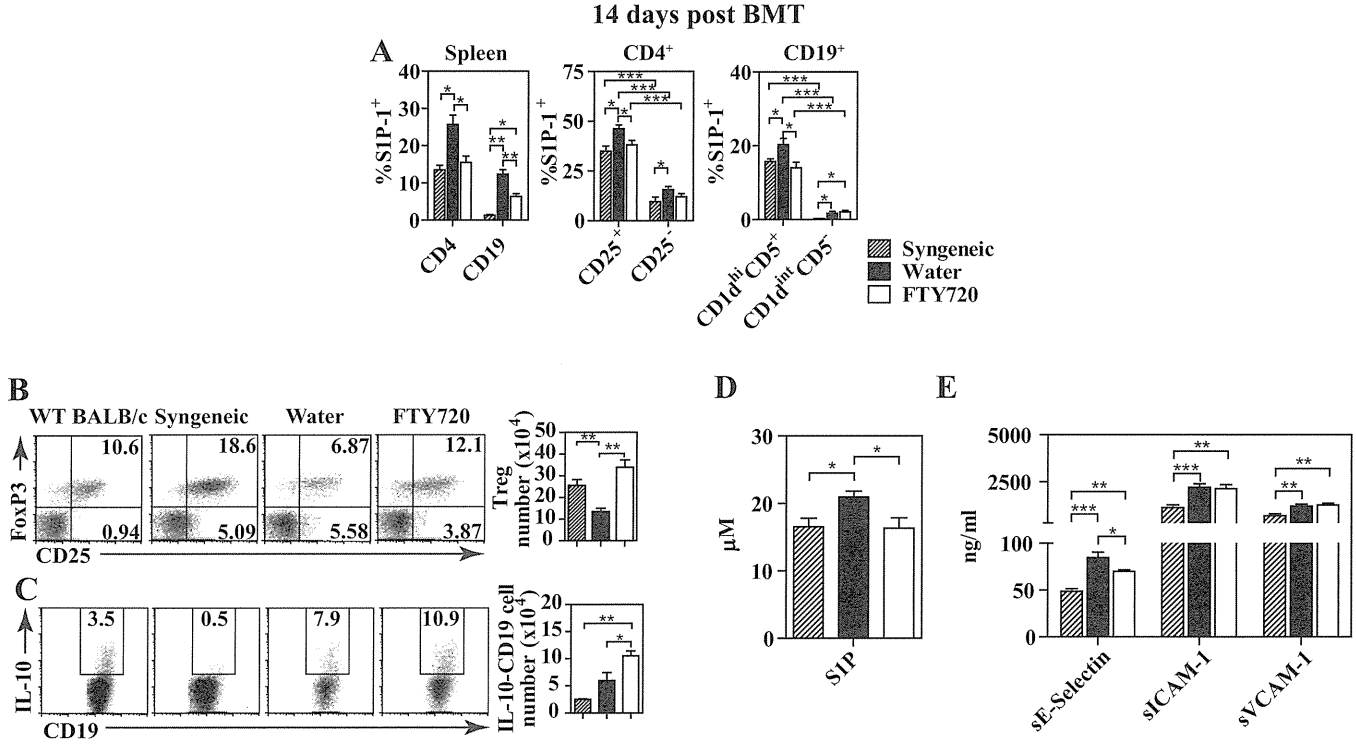

Figure 4. Early FTY720 treatment promotes expansion of Treg and Breg cells in the spleen via sphingosine 1-phosphate receptor 1 ($S1P_1$) and reduces serum levels of S1P and soluble E-selectin (sE-selectin). **A,** Frequencies of $S1P_1$ expression in splenic CD4+ T cells, CD19+ B cells, and their subsets (including CD4+CD25+ T cells, CD4+CD25– T cells, CD19+CD1d^{high}CD5+ B cells, and CD19+CD1d^{intermediate}CD5– B cells) were measured by flow cytometry. Splenic Treg cells and Breg cells were analyzed as described in Materials and Methods. Values are the mean ± SEM of 4–5 mice per group. **B,** Representative results demonstrate the frequency of splenic CD25+ cells and FoxP3+ cells within the indicated gates among total CD4+ T cells (left). Numbers of splenic CD4+CD25+FoxP3+ T cells (Treg cells) analyzed 14 days after bone marrow transplantation (BMT) are also shown (right). Values are the mean ± SEM of 4–5 mice per group. **C,** Representative results demonstrate the frequency of interleukin-10 (IL-10)–positive cells within indicated gates among total CD19+ B cells (left). Numbers of splenic IL-10–producing CD19+ B cells (Breg cells) determined 14 days after BMT are also shown (right). Values are the mean ± SEM of 4–5 mice per group. Serum samples from syngeneic mice, water-treated mice, and FTY720-treated mice were obtained 14 days after BMT. **D** and **E,** Serum levels of S1P (**D**) and of soluble E-selectin, soluble intercellular adhesion molecule 1 (sICAM-1), and soluble vascular cell adhesion molecule 1 (sVCAM-1) (**E**) were measured by an S1P competitive enzyme-linked immunosorbent assay kit and by Quantikine mouse soluble E-selectin, sICAM-1, and sVCAM-1 immunoassay kits, respectively. Values are the mean ± SEM of 5–7 mice per group. * = $P < 0.05$; ** = $P < 0.01$; *** = $P < 0.001$. WT BALB/c = wild-type BALB/c mice (without BMT).

Treg and Breg cells were higher in the FTY720-treated group ($P = 0.0015$ for Treg cells and $P = 0.0497$ for Breg cells) (Figures 4B and C). FTY720 treatment regulated expression of $S1P_1$ on CD4+CD25+ T cell and CD19+CD1d^{high}CD5+ B cell subsets to promote expansion of Treg and Breg cells in spleen.

Early FTY720 treatment normalizes elevated serum S1P and soluble E-selectin levels. To investigate elevated S1P levels and the effects of S1P on vascular damage, serum samples were obtained 14 days after BMT and levels of S1P, soluble E-selectin, sICAM-1, and sVCAM-1 were analyzed using ELISA. Fourteen days post-BMT, serum levels of S1P, soluble E-selectin, sICAM-1, and sVCAM-1 were significantly elevated in allogeneic BM-transplanted mice as compared with syngeneic mice ($P = 0.024$, $P = 0.0004$, $P = 0.0007$, and $P = 0.007$, respectively) (Figures 4D and E). FTY720 treatment reduced serum levels of S1P and soluble E-selectin, but had no influence on sICAM-1 and sVCAM-1.

FTY720 treatment reduces early infiltration of CD4+ T cells and inhibits the migration of other immune cells into the skin, resulting in decreased expression levels of $S1P_1$ in the skin. Infiltration of CD4+ T cells was elevated 7 days after allogeneic BMT as compared with syngeneic BMT ($P = 0.01$)

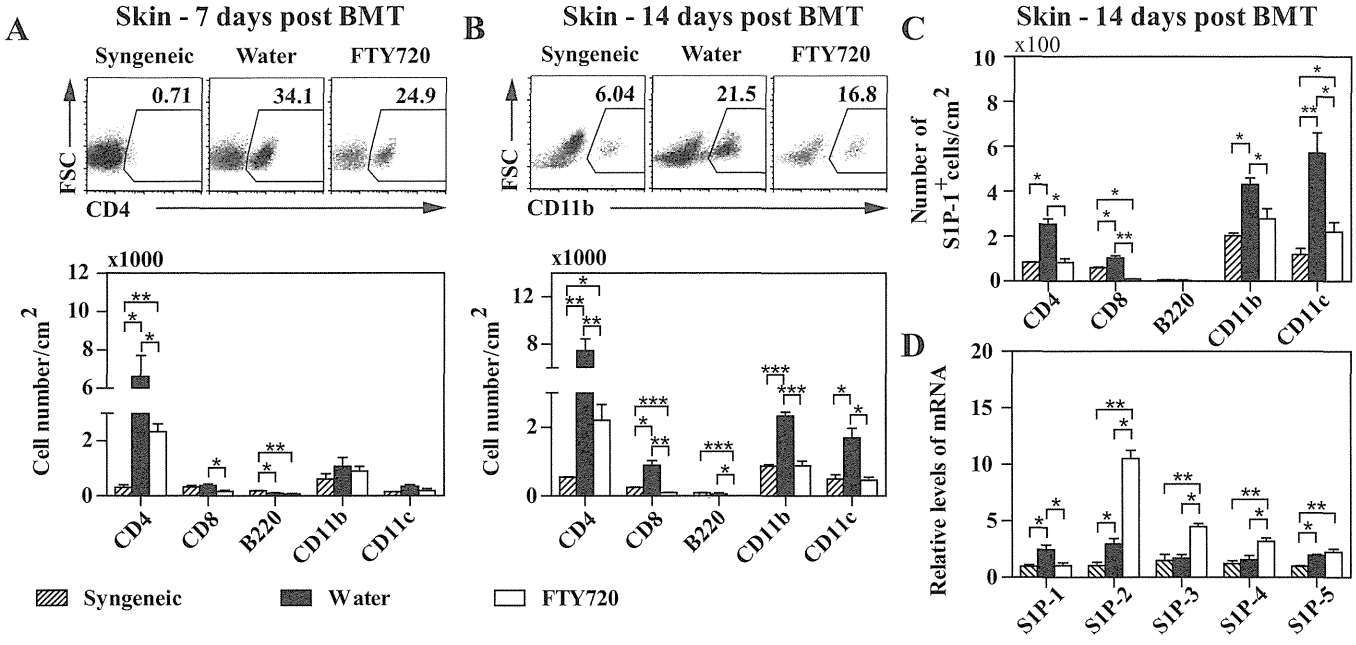

Figure 5. FTY720 treatment reduces early infiltration of immune cells into skin after BMT, resulting in decreased expression of $S1P_1$. Skin cell suspensions from syngeneic mice, water-treated mice, and FTY720-treated mice were generated by digesting a 3 × 3–cm piece of depilated skin (see Materials and Methods) and were stained for surface markers and to differentiate live cells from dead cells. **A,** Representative results demonstrate the frequency of skin CD4+ cells within indicated gates among total live cells (top). Numbers of skin CD4+, CD8+, B220+, CD11b+, and CD11c+ cells 7 days after BMT are also shown (bottom). **B,** Representative results demonstrate the frequency of skin CD11b+ cells within indicated gates among total live cells (top). Numbers of skin CD4+, CD8+, B220+, CD11b+, and CD11c+ cells 14 days after BMT are also shown (bottom). **C,** Shown are the numbers of skin CD4+, CD8+, B220+, CD11b+, and CD11c+ cells with $S1P_1$ expression. **D,** Messenger RNA expression of $S1P_1$, $S1P_2$, $S1P_3$, $S1P_4$, and $S1P_5$ in the skin was measured by real-time quantitative polymerase chain reaction analysis 14 days after BMT. Values are the mean ± SEM of 4–5 mice per group. * = $P < 0.05$; ** = $P < 0.01$; *** = $P < 0.001$. See Figure 4 for definitions.

(Figure 5A). CD8+ T cells, CD11b+ monocyte/macrophages, and CD11c+ dendritic cells were increased 14 days after BMT in the water-treated group as compared with the syngeneic group ($P = 0.018$, $P = 0.0004$, and $P = 0.017$, respectively) (Figure 5B). FTY720 treatment decreased the numbers of CD4+ T cells 7 and 14 days after BMT and resulted in diminished numbers of CD8+ T cells, B220+ B cells, CD11b+ monocyte/macrophages, and CD11c+ dendritic cells 14 days post-BMT.

There was no significant difference in the percentages of $S1P_1$+ cells among skin CD4+, CD8+, B220+, CD11b+, and CD11c+ cells in the FTY720-treated group as compared with the control group (data not shown). However, FTY720 treatment reduced $S1P_1$+ CD4+, CD8+, CD11b+, and CD11c+ cells in the skin of mice with sclerodermatous chronic GVHD (Figure 5C). To investigate expression levels of S1P receptors in skin, $S1P_1$, $S1P_2$, $S1P_3$, $S1P_4$, and $S1P_5$ expression was determined by real-time RT-PCR. Although expression levels of $S1P_1$, $S1P_2$, and $S1P_5$ were increased after allogeneic BMT, FTY720 treatment suppressed $S1P_1$ expression in the skin 14 days after BMT (Figure 5D). The inhibition was due to reduced immune cell infiltration into skin after FTY720 treatment.

FTY720 reduces mRNA expression of skin cytokines/chemokines 14 days after BMT. Expression of mRNA for chemokines such as CCL2 (monocyte chemotactic protein 1 [MCP-1]), CCL3 (macrophage inflammatory protein 1α [MIP-1α]), and CCL5 (RANTES) was up-regulated in mice with sclerodermatous chronic GVHD compared with syngeneic mice 7 days after BMT (6-fold, 12-fold, and 6-fold versus syngeneic mice; $P = 0.018$, $P = 0.024$, and $P = 0.049$, respectively) and 14 days after BMT (30-fold, 430-fold, and 300-fold versus syngeneic mice; $P = 0.014$, $P = 0.015$, and $P = 0.0012$, respectively). However, expression of chemokine mRNA was decreased by FTY720 treatment 14 days after BMT (Figure 6A).

IL-6 and IL-10 mRNA expression levels were up-regulated 7 days after BMT (6.5-fold and 38-fold versus syngeneic mice; $P = 0.027$ and $P = 0.045$, respectively) (Figure 6A). Furthermore, mRNA

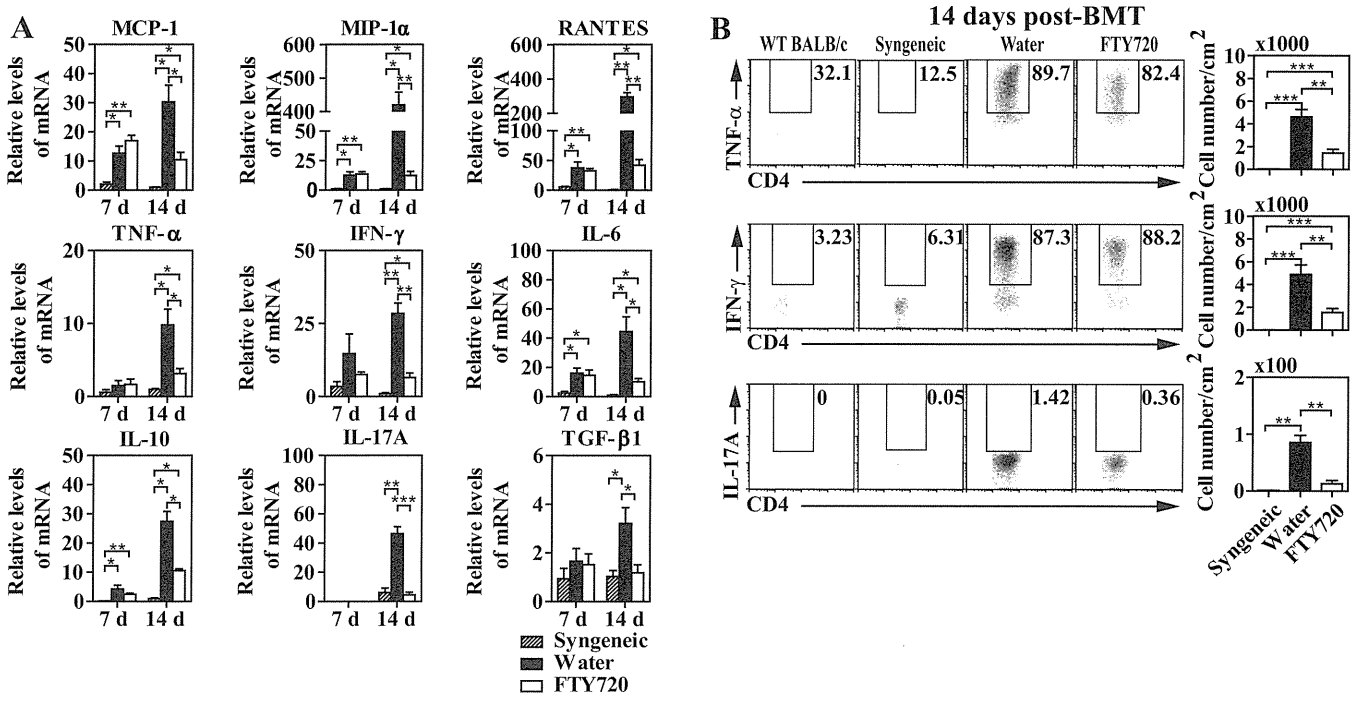

Figure 6. FTY720 inhibits skin expression of chemokines/cytokines. **A,** Expression of mRNA for monocyte chemotactic protein 1 (MCP-1), macrophage inflammatory protein 1α (MIP-1α), RANTES, tumor necrosis factor α (TNFα), interferon-γ (IFNγ), interleukin-6 (IL-6), IL-10, IL-17A, and transforming growth factor β1 (TGFβ1) in the skin was measured by real-time quantitative polymerase chain reaction analysis 7 and 14 days after BMT. **B,** Skin single-cell suspensions from WT BALB/c mice, syngeneic mice, water-treated mice, and FTY720-treated mice were cultured with phorbol myristate acetate, ionomycin, and brefeldin A for 4 hours. The culture cells were stained with anti-CD4 monoclonal antibodies, following by intracellular staining for TNFα, IFNγ, and IL-17A. Representative results demonstrate the frequency of TNFα+, IFNγ+, and IL-17A+ cells within indicated gates among total CD4+ T cells (left). Numbers of skin TNFα-, IFNγ-, and IL-17A–producing CD4+ T cells analyzed 14 days after BMT are also shown (right). Values are the mean ± SEM of 4 mice per group. * = $P < 0.05$; ** = $P < 0.01$; *** = $P < 0.001$. See Figure 4 for other definitions.

expression of TNFα, IFNγ, IL-6, IL-10, IL-17A, and transforming growth factor β1 (TGFβ1) was markedly elevated in mice with sclerodermatous chronic GVHD 14 days after BMT (10-fold, 30-fold, 43-fold, 28-fold, 8-fold, and 3-fold versus syngeneic mice; $P = 0.04$, $P = 0.004$, $P = 0.023$, $P = 0.014$, $P = 0.0007$, and $P = 0.045$, respectively) (Figure 6A). In contrast, FTY720 treatment markedly downgraded TNFα, IFNγ, IL-6, IL-10, IL-17A, and TGFβ1 (Figure 6A).

In mice with sclerodermatous chronic GVHD, the percentages of TNFα- and IFNγ-producing CD4+ T cells were high (85–95%). FTY720 treatment did not change TNFα and IFNγ production by CD4+ T cells, but inhibited the numbers of TNFα- and IFNγ-producing CD4+ T cells with diminished infiltration of CD4+ T cells into the skin. Notably, 14 days after BMT, FTY720 treatment significantly reduced the percentage of IL-17A–producing CD4+ T cells (mean ± SEM 0.51 ± 0.16% versus 1.16 ± 0.16%; $P = 0.029$) (data not shown) and the number of IL-17A–producing CD4+ T cells (mean ± SEM 12.9 ± 5.76 cells/cm^2 versus 85.2 ± 12.58 cells/cm^2; $P = 0.005$) (Figure 6B).

DISCUSSION

In this study, we demonstrated that early or delayed administration of FTY720 treatment significantly reduced the severity and fibrosis of murine sclerodermatous chronic GVHD as determined by both skin manifestation and histopathology. FTY720 treatment restored PTEN expression and normalized Smad3 phosphorylation in skin fibroblasts. PTEN deficiency has been reported to be associated with fibrosis (30). Furthermore, TGFβ1 was shown to simultaneously activate phosphorylation of the Smad3 signaling pathway in fibroblasts (31). Immunohistochemical analysis suggested that treatment with FTY720 markedly decreased the infiltration of CD3+ cells, CD4+ T cells,

and CD11b+ monocyte/macrophages into the skin 42 days after BMT. Moreover, short-term early treatment with FTY720 for 20 days at 1 mg/kg sustained the inhibition of murine sclerodermatous chronic GVHD fibrosis for 42 days after BMT, revealing that early administration of FTY720 markedly suppressed early alloreactive reactions between donor-derived immune cells and host cell populations.

MDSCs, defined as CD11b+Gr-1+ cells in mice (32), are now known to develop under various conditions characterized by immune stimulation such as trauma (33), infection (34), inflammation (35), and autoimmunity (36). MDSCs inhibited acute GVHD with limited donor T cell proliferation, activation, and proinflammatory cytokine production (37). Splenic MDSCs, elevated by treatment with FTY720 7 days post-BMT, suppressed proliferation of splenic CD4+ T cells (Figure 3). In a previous study, it was found that BM-derived monocyte/macrophages expressed higher levels of $S1P_1$ than $S1P_3$. However, S1P can induce signaling through $S1P_3$, suggesting that FTY720 not only affects monocyte/macrophage migration, but also affects activation (8).

In Treg cells, a key negative signal is delivered by $S1P_1$, mediated primarily by the Akt–mammalian target of rapamycin pathway, for the development, maintenance, and function of these cells (11). FTY720 treatment was shown to induce an increase in Treg cells in vitro and in vivo, as well as augment their suppressive activity (10). Down-regulated expression of $S1P_1$ in CD4+CD25+ T cells suggests that FTY720 treatment acts as an antagonist to $S1P_1$ in Treg cells. FTY720 phosphate can bind to $S1P_1$, resulting in the inhibition of $S1P_1$ signals. Furthermore, a previous study demonstrated that FTY720 caused displacement of MZ B cells to the splenic follicles, but increased the percentage of MZ B cells expressing the activation markers CD1d and CD24 (38). MZ B cells express more $S1P_1$ and $S1P_3$ than do follicular B cells (12,13).

The current study also showed that the $S1P_1$ level was higher in the $CD1d^{high}CD5+$ B cell population than in the $CD1d^{intermediate}CD5-$ B cell population. Moreover, increased expression of $S1P_1$ in the $CD1d^{high}$ CD5+ B cell population in control groups was inhibited by FTY720 treatment (Figure 4A). FTY720 caused $S1P_1$ to internalize on CD4+ T cells and CD19+ B cells as well as on their regulatory subsets, including CD4+ CD25+ and $CD1d^{high}CD5+$ populations, in murine sclerodermatous chronic GVHD. While both $S1P_1$ and $S1P_3$ promote MZ B cell migration in the splenic marginal zone, $S1P_3$ is essential for regulating the function and development of MZ B cells (39,40). In the current study, the presence of Treg and Breg cells capable of suppressing immune responses in murine sclerodermatous chronic GVHD was enhanced by FTY720 treatment 14 days after BMT via $S1P_1$ (Figures 4B and C).

The migration and recruitment of immune cells to a target tissue is a multistep process involving the sequential activation of various adhesion molecules on immune cells and the vascular endothelium as well as the expression of a vast array of chemokines/cytokines (41). Inflammatory cells, mast cells, platelets, and endothelial cells are ready sources of S1P in SSc patients (21). SSc patients showed significantly higher serum levels of S1P, soluble E-selectin, sVCAM-1, and sICAM-1 (19,42,43). While serum levels of S1P, soluble E-selectin, sICAM-1, and sVCAM-1 were elevated in allogeneic BM-transplanted mice 14 days post-BMT, FTY720 reduced serum levels of S1P and soluble E-selectin, but had no influence on sICAM-1 and sVCAM-1 (Figures 4D and E). Unlike other endothelial adhesion molecules, such as VCAM-1 and ICAM-1, E-selectin expression appears to be restricted to endothelial cells (43). The results demonstrated that FTY720 attenuates vascular damage in murine sclerodermatous chronic GVHD.

Previous studies indicated that FTY720 phosphate, an agonist at 4 S1P receptors, inhibited lymphocyte migration by 2 independent mechanisms: a down-modulation of $S1P_1$ on T cells resulting in a reduced response of cells to the migration signal S1P (functional antagonist), and a persistent signaling at $S1P_1$ on the sinus lining endothelium to increase barrier function and reduce transmigration of lymphocytes (agonist) (7,44,45). Otherwise, the current study demonstrated that the role of immunosuppression of regulatory cells was hypothetically down-regulated by the S1P receptor antagonist FTY720. Thus, FTY720 may differentially regulate development of murine sclerodermatous chronic GVHD in dual agonist and antagonist roles of S1P receptors.

Tissue damage causes up-regulation of inflammatory chemokines/cytokines and chemoattractants in target tissues (46–48). MCP-1, MIP-1α, and RANTES belong to the CC chemokine family and primarily attract monocytes (MCP-1, MIP-1α) and T cells (RANTES). In the current study, the expression of MCP-1, MIP-1α, and RANTES in skin was suppressed by FTY720 treatment, paralleled by a significant decrease in the numbers of CD4+ T cells, CD8+ T cells, and CD11b+ monocyte/macrophages infiltrating the skin (Figure 5B). In addition, FTY720 significantly suppressed the infiltration of

Th1 cells (TNFα- and IFNγ-producing CD4+ T cells) and Th17 cells (IL-17A–producing CD4+ T cells) at an early stage of development of murine sclerodermatous chronic GVHD (Figure 6B).

TNFα is a proinflammatory cytokine that plays a role in all phases of chronic GVHD pathophysiology, mediating both direct tissue damage and indirect tissue damage caused by lymphocytes (49). An imbalance between the Th1 and Th2 cytokines might be important in the pathogenesis of scleroderma (50). Further, MCP-1 and RANTES may play a role in the fibrotic pathway by modulating collagen turnover or type I and IV collagen deposition directly to fibroblasts via monocyte/macrophages, or indirectly through TGFβ. In skin, FTY720 treatment reduced TGFβ1 to levels found in syngeneic animals (Figure 6A). It is hypothesized that monocyte activation by host-reactive T cells is an initiating event in scleroderma and human sclerodermatous chronic GVHD. Infiltrating monocytes in the skin produce TGFβ1, resulting in decreased PTEN levels and up-regulation of Smad3 phosphorylation and collagen and leading to skin fibrosis (20,46).

In conclusion, we have demonstrated that both early and delayed administration of FTY720 treatment effectively reduces severity and fibrosis of murine sclerodermatous chronic GVHD. FTY720 suppressed the immune response by promoting the expansion of regulatory cells and by reducing vascular damage and infiltration of immune cells into skin. The current studies suggest that FTY720 is a potential candidate for use in treating patients with sclerodermatous chronic GVHD and scleroderma.

ACKNOWLEDGMENTS

We thank Ms M. Matsubara and Ms Y. Yamada for technical assistance.

AUTHOR CONTRIBUTIONS

All authors were involved in drafting the article or revising it critically for important intellectual content, and all authors approved the final version to be published. Dr. Matsushita had full access to all of the data in the study and takes responsibility for the integrity of the data and the accuracy of the data analysis.

Study conception and design. Le Huu, Matsushita, Hamaguchi, Hasegawa, Takehara, Fujimoto.

Acquisition of data. Le Huu, Matsushita, Jin.

Analysis and interpretation of data. Le Huu, Matsushita, Fujimoto.

REFERENCES

1. Cyster JG. Chemokines, sphingosine-1-phosphate, and cell migration in secondary lymphoid organs. Annu Rev Immunol 2005;23:127–59.
2. Rosen H, Goetzl EJ. Sphingosine 1-phosphate and its receptors: an autocrine and paracrine network. Nat Rev Immunol 2005;5:560–70.
3. Chiba K, Matsuyuki H, Maeda Y, Sugahara K. Role of sphingosine 1-phosphate receptor type 1 in lymphocyte egress from secondary lymphoid tissues and thymus. Cell Mol Immunol 2006;3:11–9.
4. Zemann B, Kinzel B, Muller M, Reuschel R, Mechtcheriakova D, Urtz N, et al. Sphingosine kinase type 2 is essential for lymphopenia induced by the immunomodulatory drug FTY720. Blood 2006;107:1454–8.
5. Matloubian M, Lo CG, Cinamon G, Lesneski MJ, Xu Y, Brinkmann V, et al. Lymphocyte egress from thymus and peripheral lymphoid organs is dependent on S1P receptor 1. Nature 2004;427:355–60.
6. Chiba K, Yanagawa Y, Masubuchi Y, Kataoka H, Kawaguchi T, Ohtsuki M, et al. FTY720, a novel immunosuppressant, induces sequestration of circulating mature lymphocytes by acceleration of lymphocyte homing in rats. I. FTY720 selectively decreases the number of circulating mature lymphocytes by acceleration of lymphocyte homing. J Immunol 1998;160:5037–44.
7. Brinkmann V, Cyster JG, Hla T. FTY720: sphingosine 1-phosphate receptor-1 in the control of lymphocyte egress and endothelial barrier function. Am J Transplant 2004;4:1019–25.
8. Keul P, Lucke S, von Wnuck Lipinski K, Bode C, Graler M, Heusch G, et al. Sphingosine-1-phosphate receptor 3 promotes recruitment of monocyte/macrophages in inflammation and atherosclerosis. Circ Res 2011;108:314–23.
9. Nofer JR, Bot M, Brodde M, Taylor PJ, Salm P, Brinkmann V, et al. FTY720, a synthetic sphingosine 1 phosphate analogue, inhibits development of atherosclerosis in low-density lipoprotein receptor-deficient mice. Circulation 2007;115:501–8.
10. Sawicka E, Dubois G, Jarai G, Edwards M, Thomas M, Nicholls A, et al. The sphingosine 1-phosphate receptor agonist FTY720 differentially affects the sequestration of $CD4^+/CD25^+$ T-regulatory cells and enhances their functional activity. J Immunol 2005;175:7973–80.
11. Liu G, Burns S, Huang G, Boyd K, Proia RL, Flavell RA, et al. The receptor S1P1 overrides regulatory T cell-mediated immune suppression through Akt-mTOR. Nat Immunol 2009;10:769–77.
12. Cinamon G, Matloubian M, Lesneski MJ, Xu Y, Low C, Lu T, et al. Sphingosine 1-phosphate receptor 1 promotes B cell localization in the splenic marginal zone. Nat Immunol 2004;5:713–20.
13. Cinamon G, Zachariah MA, Lam OM, Foss FW Jr, Cyster JG. Follicular shuttling of marginal zone B cells facilitates antigen transport. Nat Immunol 2008;9:54–62.
14. Kappos L, Antel J, Comi G, Montalban X, O'Connor P, Polman CH, et al. Oral fingolimod (FTY720) for relapsing multiple sclerosis. N Engl J Med 2006;355:1124–40.
15. Nakashima D, Kabashima K, Sakabe J, Sugita K, Kobayashi T, Yoshiki R, et al. Impaired initiation of contact hypersensitivity by FTY720. J Invest Dermatol 2008;128:2833–41.
16. Fujino M, Funeshima N, Kitazawa Y, Kimura H, Amemiya H, Suzuki S, et al. Amelioration of experimental autoimmune encephalomyelitis in Lewis rats by FTY720 treatment. J Pharmacol Exp Ther 2003;305:70–7.
17. Yanagawa Y, Masubuchi Y, Chiba K. FTY720, a novel immunosuppressant, induces sequestration of circulating mature lymphocytes by acceleration of lymphocyte homing in rats. III. Increase in frequency of CD62L-positive T cells in Peyer's patches by FTY720-induced lymphocyte homing. Immunology 1998;95:591–4.
18. Bu S, Kapanadze B, Hsu T, Trojanowska M. Opposite effects of dihydrosphingosine 1-phosphate and sphingosine 1-phosphate on transforming growth factor-β/Smad signaling are mediated through the PTEN/PPM1A-dependent pathway. J Biol Chem 2008;283:19593–602.
19. Tokumura A, Carbone LD, Yoshioka Y, Morishige J, Kikuchi M,

Postlethwaite A, et al. Elevated serum levels of arachidonoyl-lysophosphatidic acid and sphingosine 1-phosphate in systemic sclerosis. Int J Med Sci 2009;6:168–76.
20. Bu S, Asano Y, Bujor A, Highland K, Hant F, Trojanowska M. Dihydrosphingosine 1-phosphate has a potent antifibrotic effect in scleroderma fibroblasts via normalization of phosphatase and tensin homolog levels. Arthritis Rheum 2010;62:2117–26.
21. Pattanaik D, Postlethwaite AE. A role for lysophosphatidic acid and sphingosine 1-phosphate in the pathogenesis of systemic sclerosis. Discov Med 2010;10:161–7.
22. Yin Z, Carbone LD, Gotoh M, Postlethwaite A, Bolen AL, Tigyi GJ, et al. Lysophosphatidic acid-activated Cl^- current activity in human systemic sclerosis skin fibroblasts. Rheumatology (Oxford) 2010;49:2290–7.
23. Keller CD, Rivera Gil P, Tolle M, van der Giet M, Chun J, Radeke HH, et al. Immunomodulator FTY720 induces myofibroblast differentiation via the lysophospholipid receptor S1P3 and Smad3 signaling. Am J Pathol 2007;170:281–92.
24. Yamamoto T. Characteristics of animal models for scleroderma. Curr Rheumatol Rev 2005;1:101–9.
25. Claman HN, Jaffee BD, Huff JC, Clark RA. Chronic graft-versus-host disease as a model for scleroderma. II. Mast cell depletion with deposition of immunoglobulins in the skin and fibrosis. Cell Immunol 1985;94:73–84.
26. Le Huu D, Matsushita T, Jin G, Hamaguchi Y, Hasegawa M, Takehara K, et al. IL-6 blockade attenuates the development of murine sclerodermatous chronic graft-versus-host disease. J Invest Dermatol 2012;132:2752–61.
27. Anderson BE, McNiff J, Yan J, Doyle H, Mamula M, Shlomchik MJ, et al. Memory CD4+ T cells do not induce graft-versus-host disease. J Clin Invest 2003;112:101–8.
28. Tanaka C, Fujimoto M, Hamaguchi Y, Sato S, Takehara K, Hasegawa M. Inducible costimulator ligand regulates bleomycin-induced lung and skin fibrosis in a mouse model independently of the inducible costimulator/inducible costimulator ligand pathway. Arthritis Rheum 2010;62:1723–32.
29. Rivera J, Proia RL, Olivera A. The alliance of sphingosine-1-phosphate and its receptors in immunity. Nat Rev Immunol 2008;8:753–63.
30. Nho RS, Xia H, Diebold D, Kahm J, Kleidon J, White E, et al. PTEN regulates fibroblast elimination during collagen matrix contraction. J Biol Chem 2006;281:33291–301.
31. Gu L, Zhu YJ, Yang X, Guo ZJ, Xu WB, Tian XL. Effect of TGF-beta/Smad signaling pathway on lung myofibroblast differentiation. Acta Pharmacol Sin 2007;28:382–91.
32. Gabrilovich DI, Bronte V, Chen SH, Colombo MP, Ochoa A, Ostrand-Rosenberg S, et al. The terminology issue for myeloid-derived suppressor cells. Cancer Res 2007;67:425.
33. Makarenkova VP, Bansal V, Matta BM, Perez LA, Ochoa JB. $CD11b^+/Gr\text{-}1^+$ myeloid suppressor cells cause T cell dysfunction after traumatic stress. J Immunol 2006;176:2085–94.
34. Delano MJ, Scumpia PO, Weinstein JS, Coco D, Nagaraj S, Kelly-Scumpia KM, et al. MyD88-dependent expansion of an immature $GR\text{-}1^+CD11b^+$ population induces T cell suppression and Th2 polarization in sepsis. J Exp Med 2007;204:1463–74.
35. Haile LA, von Wasielewski R, Gamrekelashvili J, Kruger C, Bachmann O, Westendorf AM, et al. Myeloid-derived suppressor cells in inflammatory bowel disease: a new immunoregulatory pathway. Gastroenterology 2008;135:871–81, 881.e1–5.
36. Zhu B, Bando Y, Xiao S, Yang K, Anderson AC, Kuchroo VK, et al. $CD11b^+Ly\text{-}6C^{hi}$ suppressive monocytes in experimental autoimmune encephalomyelitis. J Immunol 2007;179:5228–37.
37. Highfill SL, Rodriguez PC, Zhou Q, Goetz CA, Koehn BH, Veenstra R, et al. Bone marrow myeloid-derived suppressor cells (MDSCs) inhibit graft-versus-host disease (GVHD) via an arginase-1–dependent mechanism that is up-regulated by interleukin-13. Blood 2010;116:5738–47.
38. Vora KA, Nichols E, Porter G, Cui Y, Keohane CA, Hajdu R, et al. Sphingosine 1-phosphate receptor agonist FTY720-phosphate causes marginal zone B cell displacement. J Leukoc Biol 2005;78:471–80.
39. Donovan EE, Pelanda R, Torres RM. S1P3 confers differential S1P-induced migration by autoreactive and non-autoreactive immature B cells and is required for normal B-cell development. Eur J Immunol 2010;40:688–98.
40. Girkontaite I, Sakk V, Wagner M, Borggrefe T, Tedford K, Chun J, et al. The sphingosine-1-phosphate (S1P) lysophospholipid receptor $S1P_3$ regulates $MAdCAM\text{-}1^+$ endothelial cells in splenic marginal sinus organization. J Exp Med 2004;200:1491–501.
41. Baggiolini M. Chemokines and leukocyte traffic. Nature 1998;392:565–8.
42. Sondergaard K, Stengaard-Pedersen K, Zachariae H, Heickendorff L, Deleuran M, Deleuran B. Soluble intercellular adhesion molecule-1 (sICAM-1) and soluble interleukin-2 receptors (sIL-2R) in scleroderma skin. Br J Rheumatol 1998;37:304–10.
43. Ihn H, Sato S, Fujimoto M, Takehara K, Tamaki K. Increased serum levels of soluble vascular cell adhesion molecule-1 and E-selectin in patients with systemic sclerosis. Br J Rheumatol 1998;37:1188–92.
44. Brinkmann V, Lynch KR. FTY720: targeting G-protein-coupled receptors for sphingosine 1-phosphate in transplantation and autoimmunity. Curr Opin Immunol 2002;14:569–75.
45. Graler MH, Goetzl EJ. The immunosuppressant FTY720 down-regulates sphingosine 1-phosphate G-protein-coupled receptors. FASEB J 2004;18:551–3.
46. Zhang Y, McCormick LL, Desai SR, Wu C, Gilliam AC. Murine sclerodermatous graft-versus-host disease, a model for human scleroderma: cutaneous cytokines, chemokines, and immune cell activation. J Immunol 2002;168:3088–98.
47. Zhou L, Askew D, Wu C, Gilliam AC. Cutaneous gene expression by DNA microarray in murine sclerodermatous graft-versus-host disease, a model for human scleroderma. J Invest Dermatol 2007;127:281–92.
48. Chu YW, Gress RE. Murine models of chronic graft-versus-host disease: insights and unresolved issues. Biol Blood Marrow Transplant 2008;14:365–78.
49. Levine JE. Implications of TNF-α in the pathogenesis and management of GVHD. Int J Hematol 2011;93:571–7.
50. Kornblum MB, Fischgrund JS, Herkowitz HN, Abraham DA, Berkower DL, Ditkoff JS. Degenerative lumbar spondylolisthesis with spinal stenosis: a prospective long-term study comparing fusion and pseudarthrosis. Spine 2004;29:726–33.

TRANSPLANTATION

Donor-derived regulatory B cells are important for suppression of murine sclerodermatous chronic graft-versus-host disease

Doanh Le Huu,[1] Takashi Matsushita,[1] Guihua Jin,[1] Yasuhito Hamaguchi,[1] Minoru Hasegawa,[1] Kazuhiko Takehara,[1] Thomas F. Tedder,[2] and Manabu Fujimoto[1]

[1]Department of Dermatology, Faculty of Medicine, Institute of Medical, Pharmaceutical and Health Sciences, Kanazawa University, Kanazawa, Japan; and [2]Department of Immunology, Duke University Medical Center, Durham, NC

Key Points

- CD19-deficient donors augmented Scl-cGVHD.
- Donor regulatory B cells suppressed Scl-cGVHD.

Chronic graft-versus-host disease (cGVHD) is an increasingly frequent cause of morbidity and mortality of allogeneic hematopoietic stem-cell transplantation. Sclerodermatous cGVHD (Scl-cGVHD) is characterized by fibrosis and autoimmune features resembling those of systemic sclerosis (SSc). Transplantation of B10.D2 bone marrow and splenocytes into irradiated BALB/c mice is an established model of human Scl-cGVHD. To examine the role of B cells in Scl-cGVHD, CD19-deficient (CD19$^{-/-}$) mice were used as donors or recipients. CD19$^{-/-}$ donors induced more severe Scl-cGVHD than wild-type donors, but use of CD19$^{-/-}$ recipients resulted in no significant differences compared with wild-type recipients. Moreover, CD19 deficiency on donor B cells resulted in the expansion of splenic interleukin (IL) -6–producing monocytes/macrophages, cytotoxic CD8^{+} T cells, and Th1 cells during the early stage of disease and increased the infiltration of T cells, TGF-β–producing monocytes/macrophages, and Th2 cells into the skin in the later stage of Scl-cGVHD. IL-10–producing regulatory B cells (B10 cells) were not reconstituted by CD19$^{-/-}$ donor cells, and early adoptive transfer of B10 cells attenuated the augmented manifestations of CD19$^{-/-}$ donor-induced Scl-cGVHD. Therefore, donor-derived B10 cells have a suppressive role in Scl-cGVHD development, warranting future investigation of regulatory B-cell–based therapy for treatment of Scl-cGVHD and SSc. (*Blood*. 2013;121(16):3274-3283)

Introduction

Graft-versus-host disease (GVHD) is the most common cause of morbidity and mortality in allogeneic hematopoietic stem-cell transplantation.[1,2] Chronic GVHD (cGVHD) is characterized by fibrosis with scleroderma-like changes and autoimmune features, and thus it resembles autoimmune diseases, including systemic sclerosis (SSc).[3] Transplantation of B10.D2 (major histocompatibility complex molecules; H-2^{d}) bone marrow (BM) and splenocytes across minor histocompatibility loci into sublethally irradiated BALB/c (H-2^{d}) recipients is a well-established animal model for human sclerodermatous cGVHD (Scl-cGVHD) and SSc.[4]

Alloreactive reactions between donor-derived immune cells and host cell populations are critical in the pathogenesis of GVHD. Donor T cells have classically been considered the main effector cells, although recent studies have suggested that B cells also play fundamental roles in GVHD.[5-8] Circulating autoantibodies are frequently detected in cGVHD patients.[9] Their direct pathogenicity remains unclear, although a recent study has demonstrated that pathogenic antibody production from germinal centers plays a causal role in development of cGVHD.[10] Furthermore, donor B cells prolong the survival of pathogenic CD4^{+} T cells.[7] Clinically, studies have demonstrated the efficacy of B-cell–targeting therapy using rituximab for cGVHD.[11,12] Collectively, B cells play pathogenic roles in the development of cGVHD through diverse mechanisms.[13] To the contrary, recent studies have clarified the protective role of regulatory B cells (Bregs) in various inflammatory and autoimmune diseases. Bregs are required for prolonged allograft survival associated with interleukin-10 (IL-10).[14] Another study indicated an increase in Bregs in kidney transplant recipients after alemtuzumab treatment.[15] In acute GVHD, host B cells have a protective effect since B-cell–deficient mice experience more severe symptoms than wild-type mice.[16] However, the role of Bregs in cGVHD remains unclear.

CD19 is a B-cell–specific, cell-surface protein that serves as a positive response regulator.[17] CD19-deficient (CD19$^{-/-}$) mice exhibit severely decreased numbers of marginal zone (MZ) B cells and B-1 cells. Specifically, CD1d^{hi}CD5^{+} B cells, a fraction containing potent IL-10–producing B cells (B10 cells), are nearly absent in CD19$^{-/-}$ mice.[18,19] Furthermore, B10 cells can promote tolerogenic immune responses through IL-10–dependent mechanisms.[19-25] Contact hypersensitivity, experimental autoimmune encephalomyelitis, lupus, and inflammatory bowel diseases are augmented in CD19$^{-/-}$ mice due to the lack of B10 cells.[18,19,24,26,27] In this study, we investigated the role of Bregs in Scl-cGVHD using CD19$^{-/-}$ mice.

Methods

Mice

BALB/c and B10.D2 mice were purchased from Japan SLC (Shizuoka, Japan). CD19$^{-/-}$ mice were generated as described[28] and backcrossed onto

Submitted November 2, 2012; accepted February 9, 2013. Prepublished online as *Blood* First Edition paper, February 19, 2013; DOI 10.1182/blood-2012-11-465658.

The publication costs of this article were defrayed in part by page charge payment. Therefore, and solely to indicate this fact, this article is hereby marked “advertisement” in accordance with 18 USC section 1734.

the BALB/c or B10.D2 background for ≥12 generations. Mice were housed in a specific pathogen-free barrier facility. The Committee on Animal Experimentation of Kanazawa University Graduate School of Medical Science approved all studies and procedures.

BM transplantation

Male wild-type or $CD19^{-/-}$ B10.D2 mice and female wild-type or $CD19^{-/-}$ BALB/c mice (8 to 12 weeks old) were used as donors and recipients, respectively. BM was T-cell–depleted (TCD) with anti-CD90.2 microbeads (Miltenyi Biotec, Auburn, CA). Splenic T and B cells were isolated with anti-CD90.2 and anti-B220 microbeads (Miltenyi Biotec), respectively. Recipients were irradiated with 800 cGy (MBR-1520R; Hitachi, Tokyo, Japan) and were injected with 10×10^6 TCD BM cells, 5×10^6 splenic T cells, and 5×10^6 splenic B cells in 0.5 mL of phosphate-buffered saline to generate Scl-cGVHD. Control groups received donor cells from BALB/c (syngeneic bone marrow transplantation [BMT]) or B10.D2 mice (allogeneic BMT). All studies were approved by the institutional review board.

GVHD skin score

Clinical cGVHD score was previously described[29]: healthy appearance = 0; skin lesions with alopecia ≤1 cm^2 in area = 1; 1 to 2 cm^2 = 2; 2 to 5 cm^2 = 3; 5 to 10 cm^2 = 4; 10 to 15 cm^2 = 5; 15 to 20 cm^2 = 6; >20 cm^2 = 7. Additionally, animals were assigned 0.4 points for skin disease (lesions or scaling) on tail and 0.3 points each for lesions on ears and paws (minimum score = 0, maximum score = 8). Final scores for dead animals were kept in the data set for the remaining time points.

Histologic analysis

The skin and lung were fixed in 10% formalin and embedded in paraffin. Sections (6 μm thick) were stained with hematoxylin and eosin and Masson's trichrome. Skin histopathology was scored by a dermatopathologist (blinded to experimental groups) on the basis of epidermal interface changes, dermal collagen thickness, mononuclear cell inflammation, subdermal fat loss, and follicular dropout, with scores from 0 to 2 for each category (total score, 0 to 10).[30] Masson's trichrome staining was used to detect the collagen fibers and collagen deposition. Collagen deposition was quantified on trichrome-stained sections as the ratio of blue-stained area to total stained area by using Adobe Photoshop CS4 analysis tools.

Flow cytometry

The following monoclonal antibodies (mAbs) were used: FITC-, PE-, PE-Cy5-, PE-Cy7-, PerCP-Cy5.5-, APC-, APC-PECy7-, or Pacific Blue-conjugated mAbs to mouse Thy1.2 (30-H12), B220 (30-F11), CD4 (RM4-5), CD8 (53-6.7), CD11b (M1-70), CD19 (1D3), CD1d (1B1), CD5 (30-H12), and CD21 (7G6) (BioLegend, San Diego, CA), and Ly9.1 (30C7) (BD Biosciences, San Jose, CA). LIVE/DEAD Fixable Aqua Dead cell (Invitrogen, Grand Island, NY) was used to detect dead cells.

Splenic and skin single-cell suspensions were stained for 20 minutes for multicolor immunofluorescence analysis by using mAbs at predetermined optimal concentrations on a FACSCanto II flow cytometer (BD Biosciences).[29] Data were analyzed using FlowJo software (Tree Star, Ashland, OR).

Intracellular cytokine staining

B cells and monocytes/macrophages were stimulated for 5 hours with lipopolysaccharide (LPS; 10 μg/mL; Sigma-Aldrich, St. Louis, MO), phorbol myristate acetate (PMA; 50 ng/mL; Sigma-Aldrich), ionomycin (500 ng/mL; Sigma-Aldrich), and brefeldin A (3 μM; BioLegend) for detection of cytokine production. T cells were stimulated for 4 hours with PMA (50 ng/mL), ionomycin (1 μg/mL), and brefeldin A (3 μM). After cell-surface staining, the cells were washed, fixed, and permeabilized using the Cytofix/Cytoperm Kit (BD Biosciences), followed by staining with anti-IL-10 (JES5-16E3) or anti-IL-6 (MP5-20F3) mAbs (BioLegend), or anti–tumor necrosis factor alpha (TNF-α) (MP6-XT22), anti–interferon gamma (IFN-γ; XMG1.2), anti-IL-17A (TC11-18H10.1), or anti-granzyme B (GB11) mAbs (BioLegend) or anti-IL-13 (eBio13A) mAb (eBioscience, San Jose, CA). Skin single-cell suspensions without stimulation were stained with anti-CD11b mAb, followed by intracellular staining with anti–latency-associated peptide (LAP) mAb (TW7-16B4; BioLegend).

Cell sorting and adoptive transfer experiments

Wild-type B10.D2 mice were used as B-cell donors. Splenic B cells were first enriched by using CD19 mAb-coated microbeads (Miltenyi Biotec). In addition, $CD1d^{hi}CD5^+$ and $CD1d^{low}CD5^-$ ($CD1d^{lo}CD5^-$) B cells were isolated by using a JSAN Desktop Cell Sorter (Bay Bioscience, Kobe, Japan) with purities of 85% to 90%. After purification, 1×10^6 cells were immediately transferred intravenously into recipients.

In vitro T-cell, B-cell, and monocyte/macrophage coculture assays

Splenic B cells were stimulated with LPS (10 μg/mL) for 1 hour. $CD11b^+$ cells were isolated by CD11b mAb-coated microbeads (Miltenyi Biotec) from spleens of $CD19^{-/-}$ donor-transplanted mice 14 days after BMT. LPS-stimulated B cells (1×10^6) were cocultured with 1×10^6 $CD11b^+$ cells for 24 hours, with LPS (10 μg/mL), PMA (50 ng/mL), ionomycin (500 ng/mL), and brefeldin A (3 μM) added during the final 5 hours of culture.

Splenic $CD1d^{hi}CD5^+$ or $CD1d^{lo}CD5^-$ B cells were stimulated with LPS (10 μg/mL) for 5 hours. T cells were purified by a magnetically activated cell sorter from spleens of $CD19^{-/-}$ donor-transplanted mice 14 days after BMT, and labeled with carboxyfluorescein succinimidyl ester (CFSE). TCD splenocytes from wild-type BALB/c mice were irradiated with 3,000 cGy. CFSE-labeled T cells (4×10^5 cells/mL) and irradiated TCD splenocytes (4×10^5 cells/mL) were cultured alone or with LPS-stimulated $CD1d^{hi}CD5^+$ or $CD1d^{lo}CD5^-$ B cells (4×10^5 cells/mL) in the presence of anti-CD3 (0.5 μg/mL; BioLegend) and anti-CD28 (0.5 μg/mL; BioLegend) mAbs for 72 hours. Proliferation was measured by CFSE dilution. For cytokine analysis, T cells were cocultured as above for 72 hours, with PMA (50 ng/mL), ionomycin (1000 ng/mL), and brefeldin A (3 μM) added during the final 4 hours of culture, followed by intracellular cytokine staining.

Cytometric bead array

$CD11b^+$ cells and T cells were cocultured as described above and with recombinant IL-10 (0.5 ng/mL; BioLegend) or anti-mouse IL-10 receptor (IL-10R) mAb (30 μg/mL; 1B1.3e; BioLegend), followed by adding LPS, PMA, and ionomycin during the final 5 hours or PMA and ionomycin during the final 4 hours for $CD11b^+$-cell coculture or T-cell coculture, respectively. Cytokine concentrations in supernatant were measured by cytometric bead array inflammatory kit (BD Biosciences).

Statistics

All data are shown as mean ± standard error of the mean. The significance of differences between sample means was determined with the Student *t* test.

Results

Increased percentage of $CD1d^{hi}CD5^+$ cells and B10 cells during Scl-cGVHD development

To examine changes in splenic immune cells, T cells, monocytes/macrophages, and B cells were analyzed in syngeneic and allogeneic BMT by flow cytometry every 7 days after BMT. The percentage of $Thy1.2^+$ T cells decreased gradually after 7 days (Figure 1A), and the ratio of $CD8^+$:$CD4^+$ T cells was increased beginning 14 days after BMT in the allogeneic BMT group (Figure 1D). The splenic $CD11b^+$ monocyte/macrophage population was markedly expanded in the early stage (days 7 and 14) and in the later stage (days 35 and 42) of GVHD (Figure 1B). A lower percentage and number of B cells were

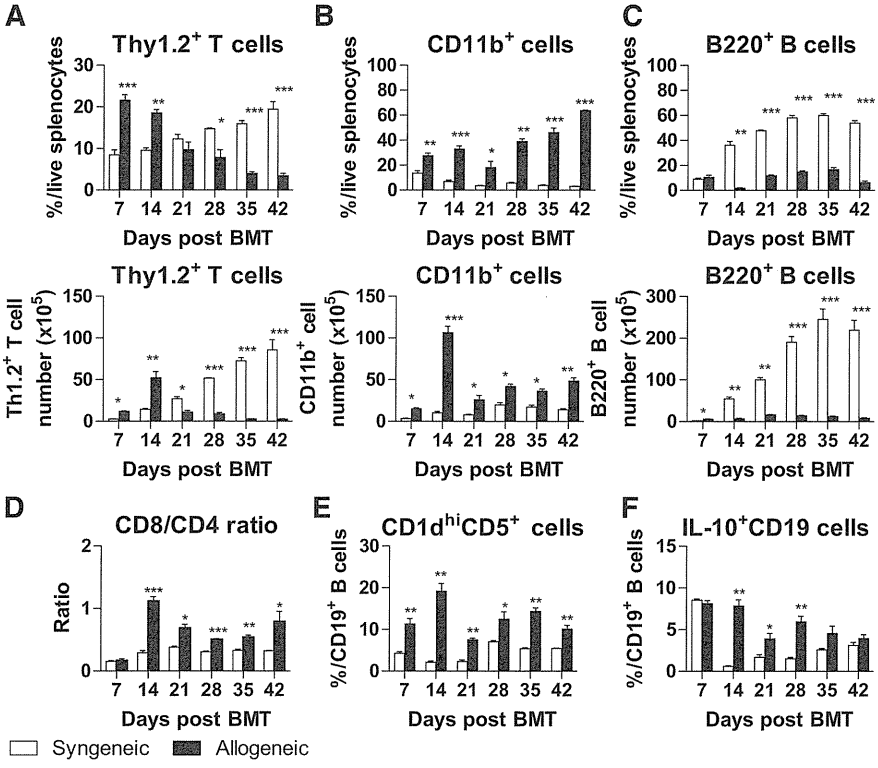

Figure 1. Changes in splenic immune cells during Scl-cGVHD development. Female BALB/c recipients were irradiated (800 cGy) and transplanted with 10×10^6 TCD BM cells and 10×10^6 unfractionated splenocytes from either male B10.D2 (allogeneic) or male BALB/c (syngeneic) donors. Spleen samples were collected every 7 days after BMT. Single-cell suspensions were stained for surface markers and to differentiate live cells from dead cells. (A) Percentage and number of Thy1.2$^+$ T cells among total live splenocytes, (B) percentages and numbers of CD11b$^+$ monocytes/macrophages among total live splenocytes, (C) B220$^+$ B cells among total live splenocytes, (D) ratio of CD8$^+$:CD4$^+$ T cells, and (E) percentage of CD1d^{hi}CD5$^+$ among (F) CD19$^+$ B cells analyzed every 7 days after BMT by flow cytometry. Splenic single-cell suspensions were cultured with PMA, ionomycin, LPS, and brefeldin A for 5 hours. B10 cell (splenic IL-10–producing B cells) frequencies were determined by intracellular staining with IL-10; 3 to 5 mice per group. *$P < .05$; **$P < .01$; ***$P < .001$.

present in allogeneic BMT mice compared with syngeneic BMT mice (Figure 1C). In comparison with syngeneic BMT, the percentage of CD1d^{hi}CD5$^+$ B cells was significantly increased after allogeneic BMT (Figure 1E). Similarly, frequencies of splenic IL-10–producing B cells (B10 cells) were also significantly elevated on days 14, 21, and 28 (Figure 1F). Thus, CD1d^{hi}CD5$^+$ B cells and B10 cells were increased during Scl-cGVHD development.

Augmented GVHD severity and fibrosis scores in CD19$^{-/-}$ donor-transplanted recipients

As described previously,[18,19] the numbers of IL-10–producing B cells were markedly decreased in CD19$^{-/-}$ mice on BALB/c and B10.D2 backgrounds compared with their wild-type counterparts ($P < .01$; Figure 2A). To investigate whether CD19 deficiency on B cells of recipients or donors has effects on Scl-cGVHD, CD19$^{-/-}$ BALB/c or CD19$^{-/-}$ B10.D2 mice were used as recipients or donors, respectively. When compared with the control group, there was no significant difference in skin score (Figure 2B), histopathologic skin score (Figure 2C), or fibrosis areas in the skin and lung (Figure 2D-E) in the CD19$^{-/-}$ recipient group. Thus, CD19 expression in recipients did not influence Scl-cGVHD. By contrast, CD19$^{-/-}$ donor cells significantly promoted Scl-cGVHD as evidenced by an increased average skin score compared with the control group ($P < .01$ and $P < .05$ on days 21 and 42, respectively; Figure 2F). Histopathologic skin scores and fibrosis areas in the skin and lungs in the CD19$^{-/-}$ donor-transplanted group were consistently significantly higher than in the control group ($P < .05$; Figure 2G-I). Therefore, CD19 deficiency in donors, but not in recipients, augmented Scl-cGVHD.

Splenic MZ, CD1d^{hi}CD5$^+$, and Bregs are decreased in CD19$^{-/-}$ donor-transplanted GVHD mice

We further analyzed the numbers of splenic B cells, MZ B cells, CD1d^{hi}CD5$^+$ B cells, and B10 cells during Scl-cGVHD development. Ly9.1$^+$ host B cells were found at low frequencies in both CD19$^{+/+}$ and CD19$^{-/-}$ transplanted groups (2.23% ± 0.01% vs 2.10% ± 0.02%, not significant; Figure 3A), suggesting that the majority of B cells are composed of donor B cells. During the early stage, the number of B220$^+$ B cells remained unchanged in CD19$^{+/+}$ and CD19$^{-/-}$ donor-transplanted groups, whereas it was significantly increased in CD19$^{+/+}$ donor-transplanted recipients during the later stage ($P < .001$ and $P < .05$ on days 21 and 42, respectively; Figure 3B).

Although there were no significant differences in the numbers of CD1d$^+$CD21$^+$ MZ and CD1d^{hi}CD5$^+$ B cells between the two groups on day 7, the development of MZ B cells and CD1d^{hi} CD5$^+$ B cells was significantly suppressed in CD19$^{-/-}$ donor-transplanted mice in both the early and late stages of Scl-cGVHD ($P < .05$; Figure 3C-D). The most remarkable difference was observed in B10 cells, since the number of B10 cells in CD19$^{-/-}$ donor-transplanted mice was significantly lower than in CD19$^{+/+}$ donor-transplanted mice (Figure 3E). Splenic B10 frequencies were also significantly lower in CD19$^{-/-}$ donor-transplanted mice when compared with CD19$^{+/+}$ donor-transplanted mice. Among B220$^+$ cells, the percentages of IL-10–producing B cells were 0.75% ± 0.24% and 0.43% ± 0.08% in CD19$^{-/-}$ donor-transplanted mice, and 9.19% ± 0.96% and 4.28% ± 0.61% in CD19$^{+/+}$ donor-transplanted group, on days 14 and 21, respectively ($P < .05$; data not shown). Collectively, disturbed reconstitution of Bregs in CD19$^{-/-}$ donor-transplanted mice may augment Scl-cGVHD.

Increased splenic T cells and cytotoxic CD8$^+$ T cells, and reduced IL-6–producing monocytes and Th1 cells in CD19$^{-/-}$ donor-transplanted GVHD mice during the early stage

The course of Scl-cGVHD can be divided into early (cytotoxic: before day 20 of BMT) and later (sclerotic: after day 20) stages.[31,32] When compared with the control group, increased frequency of Thy1.2$^+$

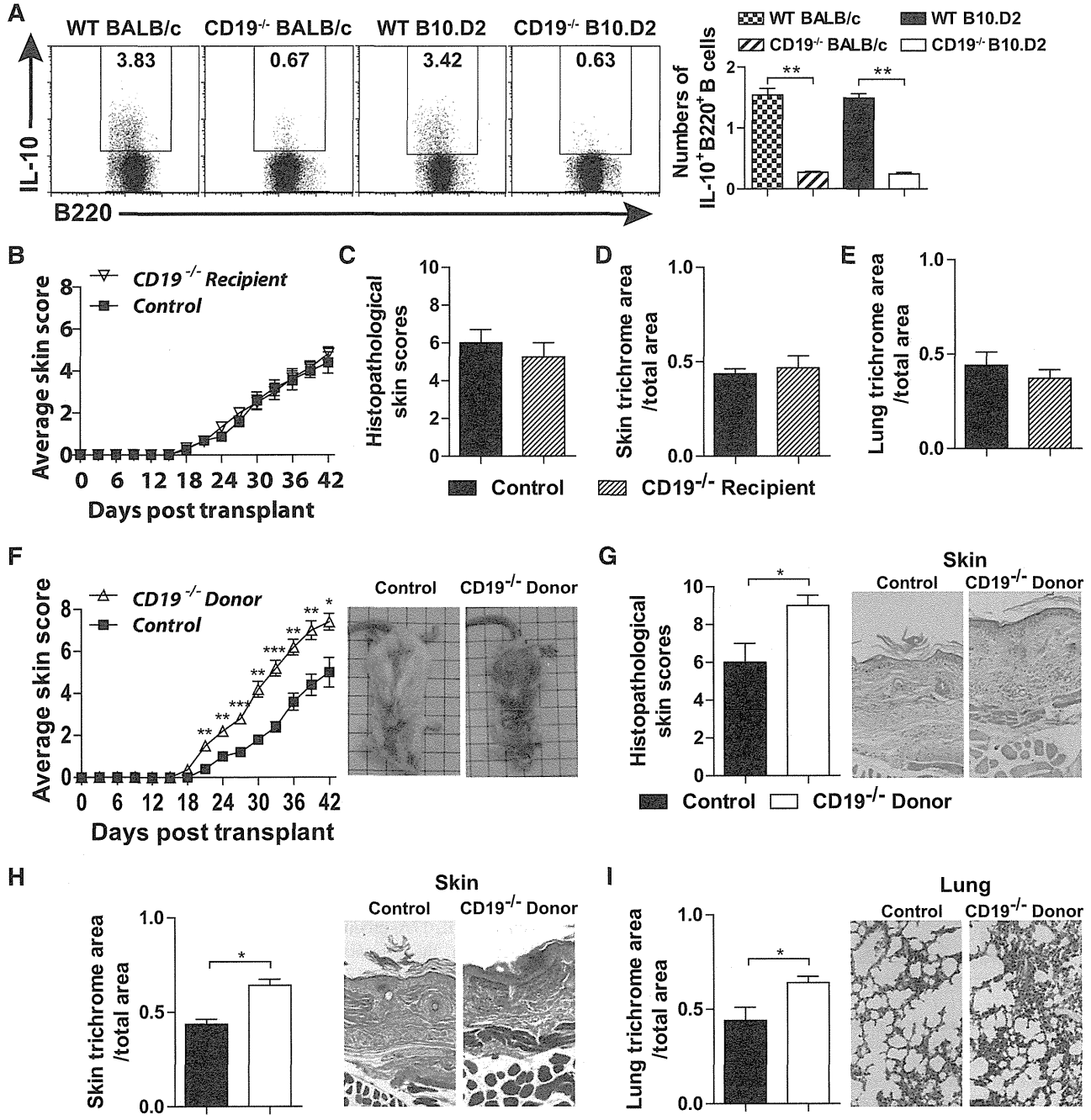

Figure 2. Augmented GVHD severity and fibrosis scores in $CD19^{-/-}$ donor-transplanted recipients. (A) Representative histograms and numbers of IL-10–producing $B220^+$ B cells in wild-type (WT) BALB/c, $CD19^{-/-}$ BALB/c, WT B10.D2, and $CD19^{-/-}$ B10.D2 groups (three mice in each group). (B) Female wild-type BALB/c (■, Control) or $CD19^{-/-}$ BALB/c (▽, $CD19^{-/-}$ Recipient) mice were transplanted with TCD BM and splenic T and B cells from wild-type $CD19^{+/+}$ B10.D2 mice. (C) Skin scores were monitored every 3 days after BMT. Histopathologic scores and the ratio of trichrome area:total area in (D) the skin and in (E) the lung were analyzed 42 days after BMT. (F) Female wild-type BALB/c mice were transplanted with TCD BM and splenic T cells and B cells from male wild-type B10.D2 (■, Control) or $CD19^{-/-}$ B10.D2 (△, $CD19^{-/-}$ Donor) mice. Skin scores were monitored every 3 days after BMT. (G) Histopathologic scores and the ratio of trichrome area:total area in (H) the skin and in (I) the lung were evaluated 42 days after BMT. Representative photographs and microphotographs were taken 42 days after BMT; 4 to 6 mice per group. $^*P < .05$; $^{**}P < .01$; $^{***}P < .001$.

T cells (Figure 4A), number of splenic $Thy1.2^+$ T cells, and a higher ratio of $CD8^+$:$CD4^+$ T cells were observed in the early stage of $CD19^{-/-}$ donor-transplanted mice ($P < .01$; Figure 4B-C). The frequency of granzyme B–producing $CD8^+$ T cells in total T cells was significantly higher in $CD19^{-/-}$ donor-transplanted mice when compared with that in $CD19^{+/+}$ donor-transplanted mice (Figure 4D). Therefore, $CD8^+$ T cells, especially granzyme B–producing cytotoxic $CD8^+$ T cells, were increased in $CD19^{-/-}$ donor-transplanted mice.

IL-6 plays an important role in the pathogenesis of Scl-cGVHD.[29] We noted elevated expansion of splenic monocytes/macrophages ($CD11b^+$ cells) in allogeneic BMT mice (Figure 1B). On day 14 after BMT, $CD11b^+$ cells produced IL-6 at a higher rate than $CD11b^-$ cells in both groups (Figure 4E). There was a significantly higher percentage of IL-6–producing $CD11b^+$ cells among total splenocytes in $CD19^{-/-}$ donor-transplanted mice compared with $CD19^{+/+}$ donor GVHD mice ($P < .05$; Figure 4F). Furthermore, $CD19^{+/+}$ donor-transplanted mice showed significantly reduced percentages of

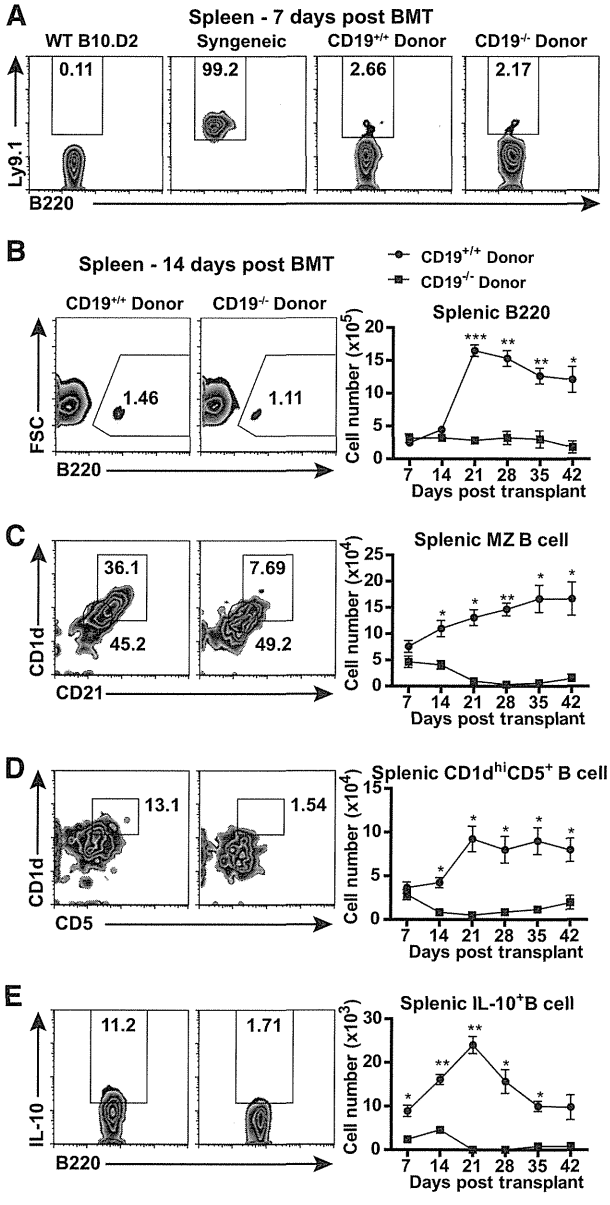

Figure 3. Decreased splenic regulatory B cells in CD19$^{-/-}$ donor-transplanted GVHD mice. Female wild-type BALB/c recipients were irradiated (800 cGy) and transplanted with TCD BM and splenic T and B cells from male wild-type B10.D2 or CD19$^{-/-}$ B10.D2 mice. (A) Frequencies of host B cells were identified by Ly9.1. Numbers of (B) splenic B cells (B220^{+}), (C) marginal zone (MZ) B cells (CD1d^{+}CD21^{+}B220^{+}), and (D) CD1d^{high}CD5^{+} B cells (CD1d^{hi}CD5^{+}B220^{+}) were analyzed every 7 days after BMT. Splenic single-cell suspensions from CD19$^{+/+}$ and CD19$^{-/-}$ donor-transplanted GVHD groups were cultured with PMA, ionomycin, LPS, and brefeldin A for 5 hours. (E) The number of splenic IL-10–producing B220^{+} B cells (Breg cells) was determined by intracellular staining every 7 days after BMT; 4 to 5 mice per group. *$P < .05$; **$P < .01$; ***$P < .001$.

TNF-α− and IFN-γ–producing CD4^{+} T cells 14 days after BMT when compared with CD19$^{-/-}$ donor-transplanted mice ($P < .01$; Figure 4G-H).

The influence of CD19$^{+/+}$ B cells on cytokine production by CD11b^{+} cells was assessed in vitro. LPS-stimulated CD19$^{+/+}$ B cells decreased IL-6 and TNF-α production in GVHD-derived CD11b^{+} monocytes/macrophages when compared with LPS-stimulated CD19$^{-/-}$ B cells (58.3% ± 0.36% vs 66.7% ± 1.85% and 60.7% ± 1.43% vs 76.3% ± 0.88%; $P < .01$; Figure 4I) or GVHD-derived monocytes/macrophages alone (Figure 4I). The inhibitory effect of LPS-stimulated CD19$^{+/+}$ B cells on cytokine production by CD11b^{+} cells was reduced by adding anti–IL-10R mAb (Figure 4J). Furthermore, IL-10 suppressed IL-6 and TNF-α production by GVHD CD11b^{+} cells in vitro (Figure 4J). Therefore, CD19 expression by donor B cells correlates with reduced IL-6 production by monocytes/macrophages.

Increased cutaneous CD11b^{+}LAP^{+} cells in the CD19$^{-/-}$ donor-transplanted group

Th2 and profibrotic cytokines produced by infiltrating immune cells promote fibrosis in Scl-cGVHD.[31,33-35] T-cell infiltration was increased 14 days (data not shown) and 21 days after CD19$^{-/-}$ donor transplantation ($P < .01$; Figure 5A). Although donor CD4^{+} T cells are required for the initiation of cGVHD,[35] CD8^{+} T cells also contribute to progression of fibrosis in Scl-cGVHD.[36] The ratio of CD8^{+}:CD4^{+} T cells in the skin was higher in the CD19$^{-/-}$ donor-transplanted group than in the CD19$^{+/+}$ donor-transplanted group 14 days (data not shown) and 21 days after BMT ($P = .003$; Figure 5B).

Activated monocyte/macrophage-secreted transforming growth factor beta (TGF-β) is a key mediator of fibrosis.[37-39] When compared with the CD19$^{+/+}$ donor-transplanted group, the percentage and number of skin CD11b^{+}LAP^{+} cells were significantly increased in the CD19$^{-/-}$ donor-transplanted group (Figure 5C-D). Therefore, donor CD19 expression may contribute to suppression of TGF-β1–producing monocytes/macrophages in the skin.

Increased cutaneous Th2 cells in the CD19$^{-/-}$ donor-transplanted group

In Scl-cGVHD cutaneous tissue, there is a mixed Th1/Th2-like cytokine profile with a Th1-like predominance during the early stage and Th2-like profile at the later stage.[38] When compared with syngeneic BMT mice, both IFN-γ–producing CD4^{+} T cells and IL-13–producing CD4^{+} T cells were clearly increased in the skin of allogeneic BMT mice (data not shown). Nonetheless, the CD19$^{-/-}$ donor GVHD group showed a modest, but significant, decrease in the percentage of skin IFN-γ–producing CD4^{+} T cells 21 days after BMT ($P = .045$; Figure 5E). There was no significant change in the percentage of IL-17A–producing CD4^{+} T cells in either group (Figure 5F). In contrast, the percentage of IL-13–producing CD4^{+} T cells was significantly increased in the skin of the CD19$^{-/-}$ donor GVHD group 21 days after BMT ($P = .0024$; Figure 5G-H). Therefore, CD19 deficiency in donor B cells promoted Th2-cell infiltration and reduced Th1-cell infiltration in the skin in the later stage of Scl-cGVHD.

Early adoptive transfer of CD1d^{hi}CD5^{+} B cells reduces the severity of CD19$^{-/-}$ donor-induced Scl-cGVHD

The CD1d^{hi}CD5^{+} B cell population was able to produce higher levels of IL-10 than CD1d^{lo}CD5^{-} B cells (Figure 6A). To evaluate the role of IL-10–producing B cells in the course of Scl-cGVHD, splenic CD1d^{hi}CD5^{+} B cells and CD1d^{lo}CD5^{-} B cells from wild-type B10.D2 mice were transferred into CD19$^{-/-}$ donor-transplanted mice on BMT day or on day 21. Early adoptive transfer of CD1d^{hi}CD5^{+} B cells (day of BMT) reduced the skin score of CD19$^{-/-}$ donor-induced Scl-cGVHD in comparison with mice given CD1d^{lo}CD5^{-} B cells and compared with CD19$^{-/-}$ donor-transplanted mice (Figure 6B). Adoptive transfer of CD21^{hi}CD23^{lo} MZ B cells from wild-type mice was also capable of reducing the severity of Scl-cGVHD, albeit less effectively (data not shown). In contrast, there were no significant changes in skin score when CD1d^{hi}CD5^{+} B cells were transferred later (day 21; Figure 6C). Host B cells were mostly absent 14 days after BMT. However, the IL-10–producing B cells

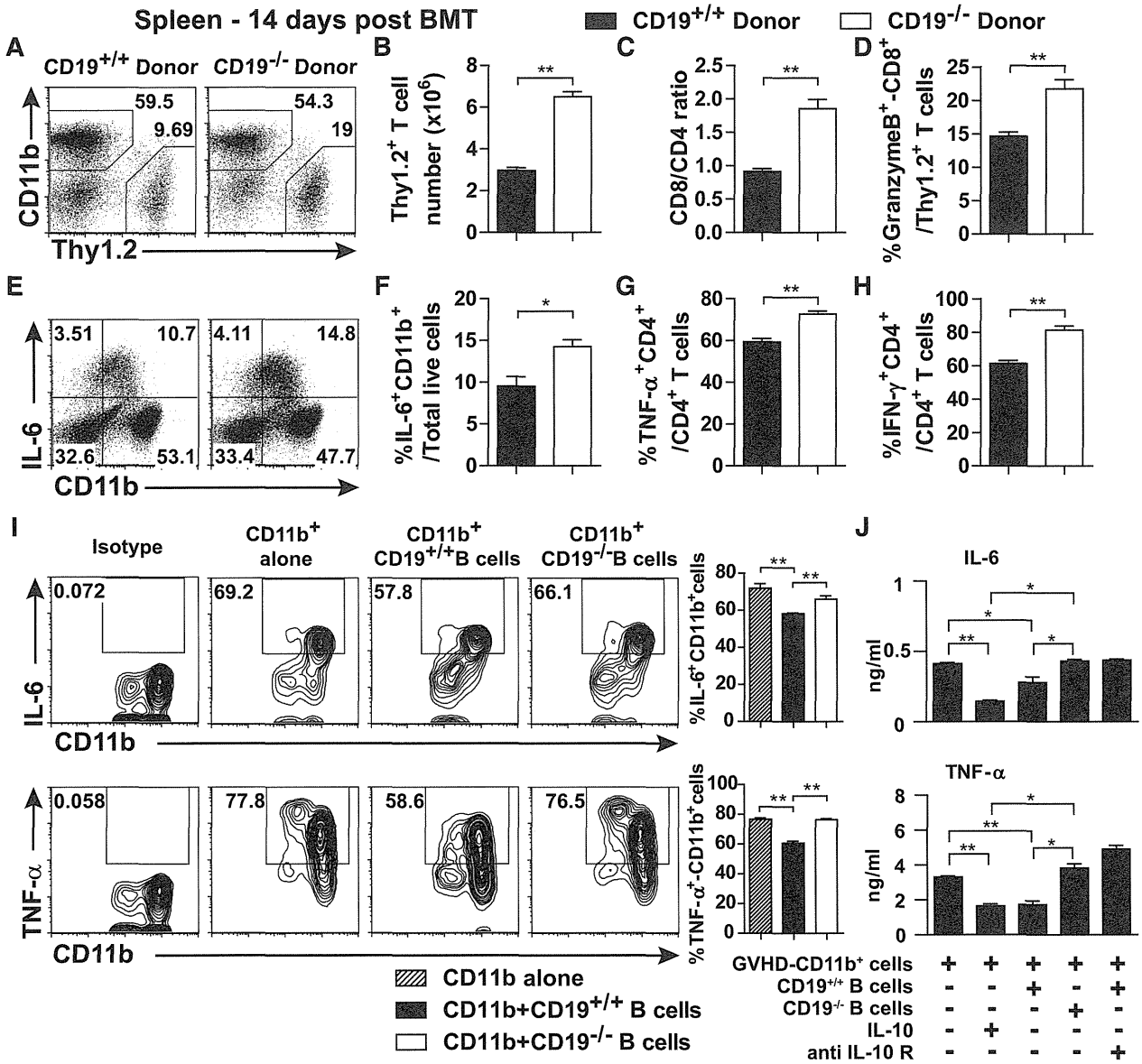

Figure 4. Splenic cytotoxic CD8$^+$ T cells, IL-6–producing CD11b$^+$ cells, and TNF-α– and IFN-γ–producing CD4$^+$ T cells are increased in CD19$^{-/-}$ donor-transplanted GVHD mice. (A) Percentages of CD11b$^+$ and Thy1.2$^+$ cells within a live gate in CD19$^{+/+}$ and CD19$^{-/-}$ donor-transplanted groups. (B) The number of splenic T cells (Thy1.2$^+$) and (C) the ratio of splenic CD8$^+$:CD4$^+$ T cells was analyzed 14 days after BMT. Splenic single-cell suspensions from CD19$^{+/+}$ donor and CD19$^{-/-}$ donor-transplanted groups were cultured with PMA, ionomycin, LPS, and brefeldin A for 5 hours for detection of IL-6–producing CD11b$^+$ cells, or with PMA, ionomycin, and brefeldin A for 4 hours for detecting granzyme B–producing CD8$^+$ T cells and TNF-α– and IFN-γ–producing CD4$^+$ T cells. (D) Percentages of cytotoxic CD8$^+$ T cells (Granzyme B–producing CD8$^+$ T cells) among T cells (Thy1.2$^+$). (E) From within a splenic live gate, percentages of CD11b$^+$ and IL-6$^+$ cells are shown in CD19$^{+/+}$ and CD19$^{-/-}$ donor-transplanted groups. (F) Percentage of IL-6–producing CD11b$^+$ cells among total live cells. (G) Percentage of TNF-α–producing CD4$^+$ T cells and (H) percentage of IFN-γ–producing CD4$^+$ T cells among CD4$^+$ T cells; 4 to 5 mice per group. *$P < .05$; **$P < .01$. LPS-stimulated B cells purified from wild-type or CD19$^{-/-}$ B10.D2 spleens were cocultured with purified CD11b$^+$ cells from CD19$^{-/-}$ donor-transplanted mice 14 days after BMT with/without IL-10 or anti–IL-10R antibody. (I) Representative histograms and bar graphs showed percentage of IL-6– or TNF-α–producing CD11b$^+$ cells from CD11b$^+$ cells. (J) Bar graphs indicate concentrations of IL-6 and TNF-α in supernatant after a 24-hour coculture. Experiments were performed in triplicate. *$P < .05$; **$P < .01$.

were significantly improved in CD1d^{hi}CD5$^+$ group when compared with CD19$^{-/-}$ donor and CD1d^{lo}CD5$^-$ groups ($P < .05$; Figure 6E). These results demonstrate that early transfer of CD1d^{hi}CD5$^+$ B cells reduces Scl-cGVHD severity due to Bregs reconstitution.

CD1d^{hi}CD5$^+$ B cells do not inhibit GVHD T-cell proliferation but do regulate T-cell IFN-γ production

To investigate the mechanisms underlying suppression of GVHD by B10 cells in vivo, T-cell/B-cell cocultures in the presence of antigen-presenting cells were performed in vitro. Incubation of GVHD T cells with B cells (CD1d^{hi}CD5$^+$ or CD1d^{lo}CD5$^-$) or without B cells did not alter T-cell proliferation (Figure 6F). By contrast, GVHD T cells cultured with CD1d^{hi}CD5$^+$ B cells showed significantly reduced IFN-γ production compared with GVHD T cells cocultured with CD1d^{lo}CD5$^-$ B cells (Figure 6G-H). The inhibitory effect of CD1d^{hi}CD5$^+$ B cells on T-cell IFN-γ production was reduced by adding anti-IL-10R mAb (Figure 6H). Furthermore, IL-10 suppressed IFN-γ production by GVHD T cells in vitro (Figure 6H).

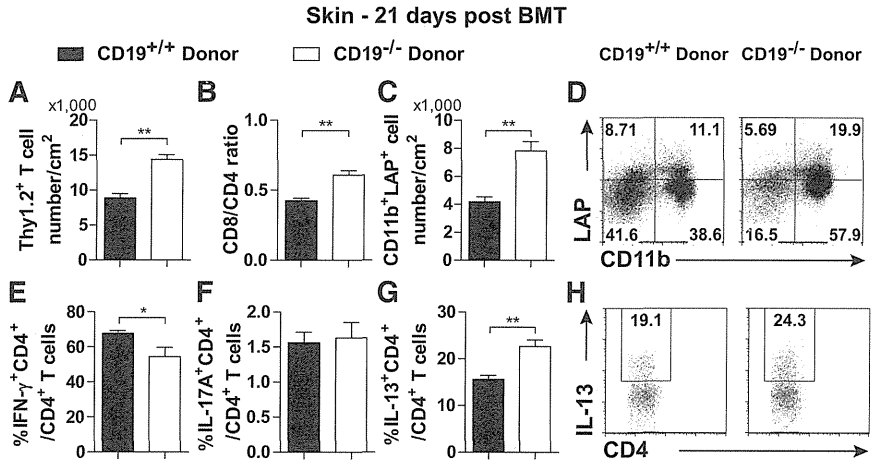

Figure 5. Increased CD11b$^+$LAP$^+$ cells and IL-13–producing CD4$^+$ T cells and reduced IFN-γ–producing CD4$^+$ T cells in the skin of CD19$^{-/-}$ donor-transplanted mice. A skin cell suspension was generated by digesting a 3 × 3-cm piece of depilated skin and was stained for surface markers and to differentiate live cells from dead cells. (A) The number of skin T cells (Thy1.2$^+$) and (B) ratio of CD8$^+$:CD4$^+$ T cells were analyzed 21 days after BMT. A skin single-cell suspension was intracellularly stained with LAP (TGF-β1). (C) The number of CD11b$^+$LAP$^+$ cells, and (D) representative histograms from a live cell gate show the percentage of CD11b$^+$LAP$^+$ cells. Skin single-cell suspensions from CD19$^{+/+}$ donor and CD19$^{-/-}$ donor-transplanted groups were cultured with PMA, ionomycin, and brefeldin A for 4 hours for detection of cytokine-producing T cells. Percentages of (E) IFN-γ–, (F) IL-17A–, and (G) IL-13–producing CD4$^+$ T cells in total CD4$^+$ T cells were analyzed. (H) Representative histograms from the CD4$^+$ gate show the percentage of IL-13–producing CD4$^+$ T cells; 4 to 5 mice per group. *$P < .05$; **$P < .01$.

Discussion

We herein demonstrate that Breg reconstitution is critical for the suppression of Scl-cGVHD. Although the percentage of splenic B cells was low during Scl-cGVHD development (Figure 1C), Breg percentages were markedly increased in wild-type donor-transplanted mice (Figure 1E-F). In contrast, the reconstitution of B10 cells was disturbed in CD19$^{-/-}$ donor-transplanted mice (Figure 3). Additionally, Scl-cGVHD severity and fibrosis were accelerated in CD19$^{-/-}$ donor-transplanted mice (Figure 2), which was lessened by adoptive transfer of CD1d^{hi}CD5$^+$ B cells from wild-type mice (Figure 6). Although a previous study indicated that host B cells suppress GVHD,[8] CD19 expression in recipients did not alter the course or severity of Scl-cGVHD (Figure 2). This study demonstrates, for the first time, that Bregs play a critical suppressive role in immune-mediated fibrotic diseases. In contrast to our study, several other studies have shown that donor B cells have disease-promoting roles in Scl-cGVHD.[5] The apparent discrepancy between the other studies and ours can be explained by the use of CD19$^{-/-}$ mice in our study, because CD19$^{-/-}$ mice are likely to have pathogenic B cells,[18,19] but they lack MZ B cells, which are major sources of B-cell–derived IL-10. Collectively, donor B cells have pathogenic and regulatory roles in the development of cGVHD.

This study indicates that an important interaction exists between B cells and CD11b$^+$ cells in Scl-cGVHD. In fact, the expansion of the monocyte/macrophage population was observed in the spleen during the early stage of disease (Figure 1B). Early blockade of IL-6 signaling by anti–IL-6 receptor mAb reduced Scl-cGVHD severity and fibrosis through an increase in regulatory T-cell numbers.[29] Our study demonstrates that IL-6 is mainly produced by splenic monocytes/macrophages (Figure 4E). Further, IL-6–producing CD11b$^+$ cells were increased in the CD19$^{-/-}$ donor-transplanted group (Figure 4F). By contrast, CD19$^{+/+}$ B cells were capable of reducing IL-6 production in CD11b$^+$ cells in vitro (Figure 4I-J). Furthermore, CD19$^{+/+}$ donor B cells were found to reduce the initial inflammatory reaction of Scl-cGVHD through B10-cell–dependent suppression of CD11b$^+$ cells. Although B10 cells have been considered to control T-cell responses, B10 cells are also likely to modulate functions of monocytes/macrophages, especially cytokine production.

Monocyte activation by host-reactive T cells is considered to be an initiating event of fibrotic changes in Scl-cGVHD.[32] Increased cutaneous T-cell infiltration was also noted in CD19$^{-/-}$ donor-transplanted mice during the early stage (Figure 5A) and may be a result of impaired suppressive functions in donor CD19$^{-/-}$ B cells. Therefore, B cells may also regulate monocyte activation indirectly via T-cell activation. Skin-infiltrating monocytes produce TGF-β1, resulting in collagen upregulation and leading to skin fibrosis.[31] TGF-β is secreted by many immune cell types, including monocytes/macrophages, in a latent form in which it is complexed with latent TGF-β binding protein, LAP.[40] Increased CD11b$^+$LAP$^+$ cell numbers were observed in the skin of CD19$^{-/-}$ donor-transplanted mice on day 21 after BMT (Figure 5C-D) and may additionally contribute to progression of skin fibrosis. Furthermore, TGF-β1 can induce the upregulation of MCP-1 and RANTES. MCP-1, in turn, can increase TGF-β secretion from macrophages.[41,42]

In addition to TGF-β, other cytokines also play pivotal roles in fibrosis. For example, IL-13, IL-10, and IL-4 released by activated T cells stimulate fibroblasts to produce collagen. In this study, IL-13–producing CD4$^+$ T cells were increased in the skin of CD19$^{-/-}$ donor-transplanted mice at the later stage (Figure 5G). In contrast, the cutaneous infiltration of IFN-γ–producing CD4$^+$ T cells was decreased in the CD19$^{-/-}$ donor-transplanted group (Figure 5E). This contrasts with the increased percentage of IFN-γ–producing CD4$^+$ T cells on day 14 in the spleens of CD19$^{-/-}$ donor-transplanted mice. It has been reported that cytokine profiles shift over the course of fibrosis in Scl-cGVHD, changing from Th1 predominance in the early phase to a Th2 profile in the later phase.[38] Thus, our finding is consistent with this profile of cytokine expression, and excessive Th2 cytokine production in the skin of CD19$^{-/-}$ donor-transplanted mice may promote fibrosis in the later stage.

Recently, B10 cells have been identified within a unique CD1d^{hi}CD5$^+$ B cell subset.[27] Although early adoptive transfer of these CD1d^{hi}CD5$^+$ B cells from wild-type B10.D2 mice into CD19$^{-/-}$ donor-transplanted mice significantly improved the average skin score, later adoptive transfer did not alter Scl-cGVHD severity (Figure 6B-C).

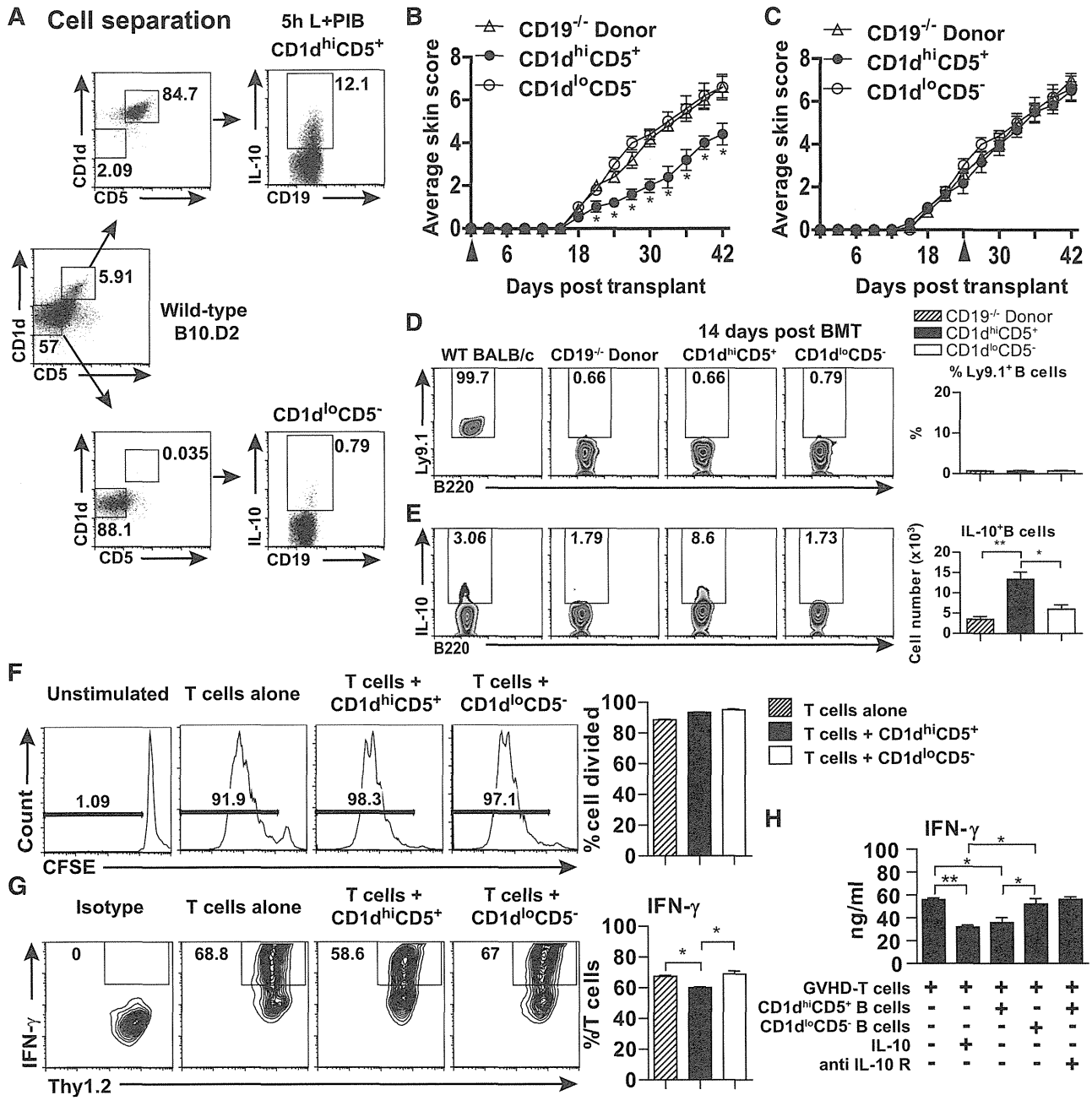

Figure 6. Early adoptive transfer of CD1d^{hi}CD5^{+} B cells reduced CD19$^{-/-}$ donor-induced Scl-cGVHD severity. (A) Representative B10-cell purification results from an adoptive transfer experiment. Purified splenic B cells from wild-type male B10.D2 were separated into CD1d^{hi}CD5^{+}CD19^{+} and CD1d^{lo}CD5^{-}CD19^{+} B-cell populations. The isolated cells were cultured with PMA, ionomycin, LPS, and brefeldin A for 5 hours. IL-10–producing B-cell frequencies in the stimulated cell cultures were determined by intracellular staining with IL-10. (B) CD19$^{-/-}$ donor-transplanted female recipients were also given phosphate-buffered saline, CD1d^{hi}CD5^{+} B cells, or CD1d^{lo}CD5^{-} B cells on the day of BMT or (C) on day 21 after BMT+- Skin scores were monitored every 3 days after BMT. (D) Percentages of host B cells (Ly.9.1^{+}B220^{+}) and (E) percentages and numbers of IL-10–producing B cells in each group are presented in representative histograms and bar graphs. (F-H) B10 cells altered the T-cell IFN-γ production profile but did not affect T-cell proliferation. (F) Representative histograms showing the proliferation of T cells when T cells and irradiated TCD splenocytes were cocultured without the presence of anti-CD3 and anti-CD28 (Unstimulated), or with the presence of anti-CD3 and anti-CD28 (T cells alone), or with either CD1d^{hi}CD5^{+} (T cells + CD1d^{hi}CD5^{+}) or CD1d^{lo}CD5^{-} (T cells + CD1d^{lo}CD5^{-}) B cells in the presence of soluble anti-CD3 and anti-CD28. Proliferation was measured by CFSE dilution. LPS-stimulated CD1d^{hi}CD5^{+} or CD1d^{lo}CD5^{-} B cells isolated from wild-type B10.D2 spleens were cocultured with purified T cells from CD19$^{-/-}$ donor-transplanted mice 14 days after BMT in presence of irradiated BALB/c TCD splenocytes and soluble anti-CD3 and anti-CD28 for 72 hours, and with/without IL-10 or anti-IL-10R antibody. (G) Representative histograms and bar graphs showed percentage of IFN-γ–producing T cells. (H) Bar graph indicates concentrations of IFN-γ in supernatant after a 72-hour coculture. The experiments were performed in triplicate. *$P < .05$; **$P < .01$.

From these results, it can be hypothesized that donor Bregs suppress the immune reaction more dominantly during the early stage than in the later stage. However, CD1d^{hi}CD5^{+} B cells from wild-type B10.D2 mice did not directly suppress GVHD-derived T-cell proliferation (Figure 6F). Instead, when these regulatory cells were cocultured with T cells, there was a significant reduction in IFN-γ (Figure 6G-H).

Although the precise mechanisms of B10 cell activation in cGVHD remain unclear, optimal expansion of B10 cells has been considered to require the initial stimulation of toll-like receptors followed by B-cell reactivity and CD40 engagements.[43] Because apoptotic cells are reported to enhance Breg functions,[44] they may serve as endogenous toll-like receptors ligands. Furthermore, a recent

study has shown that B10 cell maturation into functional IL-10–producing cells requires IL-21 and CD40-dependent cognate interactions with T cells and that IL-21 receptor and CD40 signals can efficiently drive B10 cell development and expansion in vitro,[45] suggesting the requirement of the interaction with conventional antigen-specific T cells. Conversely, recent studies have demonstrated that invariant natural killer T cells can provide cognate antigen-specific help to CD1d$^+$ B cells via CD1d and IL-21.[46,47] Additionally, increased levels of B-cell activating factor have also been reported in cGVHD.[48] B-cell activating factor treatment in vivo increases the number of B10 cells.[49] Finally, IL-10 secretion by B10 cells is likely to facilitate B10-cell expansion in an autocrine fashion. These mechanisms may collectively contribute to B10-cell expansion in the spleen in cGVHD.

In conclusion, we have demonstrated that the reconstitution of B10 cells from donor B cells exerts suppressive functions in the development of Scl-cGVHD through the reconstitution of B10 cells. Development of B10-cell–based therapy may be promising for treatment of Scl-cGVHD and other fibrotic diseases including SSc in humans.

Acknowledgments

The authors thank M. Matsubara and Y. Yamada for technical assistance.

This work was supported by grants-in-aid from the Ministry of Education, Culture, Sports, Science and Technology of Japan and from the Ministry of Health, Labour and Welfare of Japan.

Authorship

Contribution: D.L.H. designed and performed research, collected and analyzed data, and wrote the paper. T.M. designed research and collected and analyzed data and wrote the paper. G.J. performed research. Y.H., M.H., K.T., and T.F.T. designed research and wrote the paper. M.F. designed research and analyzed data and wrote the paper.

Conflict-of-interest disclosure: The authors declare no competing financial interests.

Correspondence: Takashi Matsushita, Department of Dermatology, Faculty of Medicine, Institute of Medical, Pharmaceutical and Health Sciences, Kanazawa University, Kanazawa 920-8641, Japan; e-mail: t-matsushita@derma.m.kanazawa-u.ac.jp; and Manabu Fujimoto, Department of Dermatology, Faculty of Medicine, Institute of Medical, Pharmaceutical and Health Sciences, Kanazawa University, Kanazawa 920-8641, Japan; e-mail: fujimoto-m@umin.ac.jp.

References

1. Ferrara JL, Levine JE, Reddy P, Holler E. Graft-versus-host disease. *Lancet.* 2009;373(9674):1550-1561.
2. Higman MA, Vogelsang GB. Chronic graft versus host disease. *Br J Haematol.* 2004;125(4):435-454.
3. Jaffee BD, Claman HN. Chronic graft-versus-host disease (GVHD) as a model for scleroderma. I. Description of model systems. *Cell Immunol.* 1983;77(1):1-12.
4. Yamamoto T. Characteristics of Animal Models for Scleroderma. *Curr Rheumatol Rev.* 2005;1(1):101-109.
5. Shimabukuro-Vornhagen A, Hallek MJ, Storb RF, von Bergwelt-Baildon MS. The role of B cells in the pathogenesis of graft-versus-host disease. *Blood.* 2009;114(24):4919-4927.
6. Zhang C, Todorov I, Zhang Z, et al. Donor CD4+ T and B cells in transplants induce chronic graft-versus-host disease with autoimmune manifestations. *Blood.* 2006;107(7):2993-3001.
7. Young JS, Wu T, Chen Y, et al. Donor B cells in transplants augment clonal expansion and survival of pathogenic CD4+ T cells that mediate autoimmune-like chronic graft-versus-host disease. *J Immunol.* 2012;189(1):222-233.
8. Matte-Martone C, Wang X, Anderson B, et al. Recipient B cells are not required for graft-versus-host disease induction. *Biol Blood Marrow Transplant.* 2010;16(9):1222-1230.
9. Patriarca F, Skert C, Sperotto A, et al. The development of autoantibodies after allogeneic stem cell transplantation is related with chronic graft-vs-host disease and immune recovery. *Exp Hematol.* 2006;34(3):389-396.
10. Srinivasan M, Flynn R, Price A, et al. Donor B-cell alloantibody deposition and germinal center formation are required for the development of murine chronic GVHD and bronchiolitis obliterans. *Blood.* 2012;119(6):1570-1580.
11. Sarantopoulos S, Stevenson KE, Kim HT, et al. Recovery of B-cell homeostasis after rituximab in chronic graft-versus-host disease. *Blood.* 2011;117(7):2275-2283.
12. Arai S, Sahaf B, Narasimhan B, et al. Prophylactic rituximab after allogeneic transplantation decreases B-cell alloimmunity with low chronic GVHD incidence. *Blood.* 2012;119(25):6145-6154.
13. Davis JE, Ritchie DS. B cells in GVHD: friend or foe? *Blood.* 2010;115(12):2558-2559, author reply 2559-2560.
14. Lee KM, Kim JI, Stott R, et al. Anti-CD45RB/anti-TIM-1-induced tolerance requires regulatory B cells. *Am J Transplant.* 2012;12(8):2072-2078.
15. Heidt S, Hester J, Shankar S, Friend PJ, Wood KJ. B cell repopulation after alemtuzumab induction-transient increase in transitional B cells and long-term dominance of naïve B cells. *Am J Transplant.* 2012;12(7):1784-1792.
16. Rowe V, Banovic T, MacDonald KP, et al. Host B cells produce IL-10 following TBI and attenuate acute GVHD after allogeneic bone marrow transplantation. *Blood.* 2006;108(7):2485-2492.
17. LeBien TW, Tedder TF. B lymphocytes: how they develop and function. *Blood.* 2008;112(5):1570-1580.
18. Watanabe R, Fujimoto M, Ishiura N, et al. CD19 expression in B cells is important for suppression of contact hypersensitivity. *Am J Pathol.* 2007;171(2):560-570.
19. Watanabe R, Ishiura N, Nakashima H, et al. Regulatory B cells (B10 cells) have a suppressive role in murine lupus: CD19 and B10 cell deficiency exacerbates systemic autoimmunity. *J Immunol.* 2010;184(9):4801-4809.
20. Yanaba K, Bouaziz JD, Matsushita T, Tsubata T, Tedder TF. The development and function of regulatory B cells expressing IL-10 (B10 cells) requires antigen receptor diversity and TLR signals. *J Immunol.* 2009;182(12):7459-7472.
21. DiLillo DJ, Matsushita T, Tedder TF. B10 cells and regulatory B cells balance immune responses during inflammation, autoimmunity, and cancer. *Ann N Y Acad Sci.* 2010;1183:38-57.
22. Matsushita T, Horikawa M, Iwata Y, Tedder TF. Regulatory B cells (B10 cells) and regulatory T cells have independent roles in controlling experimental autoimmune encephalomyelitis initiation and late-phase immunopathogenesis. *J Immunol.* 2010;185(4):2240-2252.
23. Iwata Y, Matsushita T, Horikawa M, et al. Characterization of a rare IL-10-competent B-cell subset in humans that parallels mouse regulatory B10 cells. *Blood.* 2011;117(2):530-541.
24. Yanaba K, Yoshizaki A, Asano Y, Kadono T, Tedder TF, Sato S. IL-10-producing regulatory B10 cells inhibit intestinal injury in a mouse model. *Am J Pathol.* 2011;178(2):735-743.
25. Yang M, Deng J, Liu Y, et al. IL-10-producing regulatory B10 cells ameliorate collagen-induced arthritis via suppressing Th17 cell generation. *Am J Pathol.* 2012;180(6):2375-2385.
26. Matsushita T, Fujimoto M, Hasegawa M, Komura K, Takehara K, Tedder TF, Sato S. Inhibitory role of CD19 in the progression of experimental autoimmune encephalomyelitis by regulating cytokine response. *Am J Pathol.* 2006;168(3):812-821.
27. Yanaba K, Bouaziz JD, Haas KM, Poe JC, Fujimoto M, Tedder TF. A regulatory B cell subset with a unique CD1dhiCD5+ phenotype controls T cell-dependent inflammatory responses. *Immunity.* 2008;28(5):639-650.
28. Engel P, Zhou LJ, Ord DC, Sato S, Koller B, Tedder TF. Abnormal B lymphocyte development, activation, and differentiation in mice that lack or overexpress the CD19 signal transduction molecule. *Immunity.* 1995;3(1):39-50.
29. Le Huu D, Matsushita T, Jin G, Hamaguchi Y, Hasegawa M, Takehara K, Fujimoto M. IL-6 blockade attenuates the development of murine sclerodermatous chronic graft-versus-host disease. *J Invest Dermatol.* 2012;132(12):2752-2761.
30. Anderson BE, McNiff J, Yan J, Doyle H, Mamula M, Shlomchik MJ, Shlomchik WD. Memory CD4+

T cells do not induce graft-versus-host disease. *J Clin Invest.* 2003;112(1):101-108.

31. Zhang Y, McCormick LL, Desai SR, Wu C, Gilliam AC. Murine sclerodermatous graft-versus-host disease, a model for human scleroderma: cutaneous cytokines, chemokines, and immune cell activation. *J Immunol.* 2002;168(6): 3088-3098.
32. Chu YW, Gress RE. Murine models of chronic graft-versus-host disease: insights and unresolved issues. *Biol Blood Marrow Transplant.* 2008;14(4):365-378.
33. McCormick LL, Zhang Y, Tootell E, Gilliam AC. Anti-TGF-beta treatment prevents skin and lung fibrosis in murine sclerodermatous graft-versus-host disease: a model for human scleroderma. *J Immunol.* 1999;163(10):5693-5699.
34. Wynn TA. Fibrotic disease and the T(H)1/T(H)2 paradigm. *Nat Rev Immunol.* 2004;4(8):583-594.
35. Hamilton BL. L3T4-positive T cells participate in the induction of graft-vs-host disease in response to minor histocompatibility antigens. *J Immunol.* 1987;139(8):2511-2515.
36. Grogan BM, Tabellini L, Storer B, et al. Activation and expansion of CD8(+) T effector cells in patients with chronic graft-versus-host disease. *Biol Blood Marrow Transplant.* 2011;17(8): 1121-1132.
37. Zhang Y, McCormick LL, Gilliam AC. Latency-associated peptide prevents skin fibrosis in murine sclerodermatous graft-versus-host disease, a model for human scleroderma. *J Invest Dermatol.* 2003;121(4):713-719.
38. Zhou L, Askew D, Wu C, Gilliam AC. Cutaneous gene expression by DNA microarray in murine sclerodermatous graft-versus-host disease, a model for human scleroderma. *J Invest Dermatol.* 2007;127(2):281-292.
39. Ihn H. Autocrine TGF-beta signaling in the pathogenesis of systemic sclerosis. *J Dermatol Sci.* 2008;49(2):103-113.
40. Khalil N. TGF-beta: from latent to active. *Microbes Infect.* 1999;1(15):1255-1263.
41. Takeshita A, Chen Y, Watanabe A, Kitano S, Hanazawa S. TGF-beta induces expression of monocyte chemoattractant JE/monocyte chemoattractant protein 1 via transcriptional factor AP-1 induced by protein kinase in osteoblastic cells. *J Immunol.* 1995;155(1):419-426.
42. Wang SN, LaPage J, Hirschberg R. Role of glomerular ultrafiltration of growth factors in progressive interstitial fibrosis in diabetic nephropathy. *Kidney Int.* 2000;57(3):1002-1014.
43. Lampropoulou V, Hoehlig K, Roch T, et al. TLR-activated B cells suppress T cell-mediated autoimmunity. *J Immunol.* 2008;180(7): 4763-4773.
44. Gray M, Miles K, Salter D, Gray D, Savill J. Apoptotic cells protect mice from autoimmune inflammation by the induction of regulatory B cells. *Proc Natl Acad Sci USA.* 2007;104(35): 14080-14085.
45. Yoshizaki A, Miyagaki T, DiLillo DJ, et al. Regulatory B cells control T-cell autoimmunity through IL-21-dependent cognate interactions. *Nature.* 2012;491(7423):264-268.
46. Chang PP, Barral P, Fitch J, et al. Identification of Bcl-6-dependent follicular helper NKT cells that provide cognate help for B cell responses. *Nat Immunol.* 2011;13(1):35-43.
47. King IL, Fortier A, Tighe M, et al. Invariant natural killer T cells direct B cell responses to cognate lipid antigen in an IL-21-dependent manner. *Nat Immunol.* 2011;13(1):44-50.
48. Allen JL, Fore MS, Wooten J, et al. B cells from patients with chronic GVHD are activated and primed for survival via BAFF-mediated pathways. *Blood.* 2012;120(12):2529-2536.
49. Yang M, Sun L, Wang S, et al. Novel function of B cell-activating factor in the induction of IL-10-producing regulatory B cells. *J Immunol.* 2010; 184(7):3321-3325.

Journal of Dermatological Science 69 (2013) 54–60

Contents lists available at SciVerse ScienceDirect

Journal of Dermatological Science

journal homepage: www.elsevier.com/jds

Circulating γ/δ T cells in systemic sclerosis exhibit activated phenotype and enhance gene expression of proalpha2(I) collagen of fibroblasts☆

Ikuko Ueda-Hayakawa [a,b,*], Minoru Hasegawa [a], Yasuhito Hamaguchi [a], Kazuhiko Takehara [a], Manabu Fujimoto [a,*]

[a] Department of Dermatology, Kanazawa University Graduate School of Medical Science, Kanazawa, Japan
[b] Department of Dermatology, Kansai Medical University, Hirakata, Japan

ARTICLE INFO

Article history:
Received 28 August 2012
Received in revised form 5 October 2012
Accepted 9 October 2012

Keywords:
Systemic sclerosis
γ/δ T cell
Fibroblast
Proalpha2(I) collagen (COL1A2)

ABSTRACT

Background: Systemic sclerosis (SSc) is a systemic inflammatory and fibrotic disease characterized by activation of circulating T lymphocytes.
Objective: To determine phenotypic abnormalities of γ/δ T cells and whether γ/δ T cells influence fibroblasts activation in SSc patients.
Methods: Number and proportion of peripheral γ/δ T lymphocytes, and their expressions of cell surface molecules were evaluated by flow cytometry. Isolated γ/δ T cells were cocultured with fibroblast, and mRNA expressions of proalpha1(I) collagen and proalpha2(I) collagen (COL1A2) of fibroblasts were analyzed by real time RT-PCR. γ/δ T cell infiltrations in the skin were examined histopathologically.
Results: No significant difference in number and proportion of γ/δ T cells was observed in SSc patients compared to healthy controls (HCs). Geometric mean fluorescence intensity (GMFI) of CD16 and CD69 on γ/δ T cells was significantly increased in patients with diffuse cutaneous SSc (dcSSc) compared to HCs. CD62L expression was significantly decreased in patients with dcSSc compared to HCs. The percentage of CD69 positive γ/δ T cells was significantly higher in patients with SSc than HCs. COL1A2 mRNA expression was significantly higher in fibroblasts cocultured with γ/δ T cells from SSc than that from HCs in cell contact independent manner. Additionally, γ/δ T cell infiltrations were observed in SSc patients' skin.
Conclusion: Our results suggest that γ/δ T cells showed activated phenotype in SSc and suggest that SSc γ/δ T cells may play an important role on fibrotic process by upregulation of COL1A2 mRNA expression in fibroblasts.

1. Introduction

Systemic sclerosis (SSc) is a systemic inflammatory and fibrotic disease characterized by activation of circulating T lymphocytes, increased levels of circulating inflammatory mediators, autoantibodies production, and typical local inflammatory infiltrates [1–5]. T cell activation is supported by the presence of $CD3^+$ T cell infiltration in the affected skin [6], and by the evidence of high concentrations of several cytokines in the patients' sera and/or in the supernatants of their cultured peripheral blood mononuclear cells (PBMC). Perivascular mononuclear cell infiltration, which is composed mainly of T lymphocytes, is seen before the onset of vascular injury and interstitial fibrosis. Fibroblast collagen production is enhanced by T helper type 2 lymphocytes (Th2) cytokines including interleukin (IL)-4 and IL-13, and inhibited by cytokines produced by Th1 cells (e.g., interferon (IFN)-γ and tumor necrosis factor (TNF)-α [7].

T cells that express αβ T cell receptor (TCR) comprise the vast majority of mature T cells in peripheral blood. In contrast, T cells that bear the γδTCR constitute a minor population of mature T cells in the circulation and lymphoid tissue. α/β and γ/δ T cells share similarities in that both differentiate primarily in the thymus, possess common cell surface antigens, and have a diversity of clonotypic receptors associated with the CD3 complex. Both α/β and γ/δ T cells fulfill unique functional roles within the immune system, however, less is known about the γ/δ T cells.

Increasing evidences suggest that γ/δ T cells influence the fibrotic process. It was reported that γ/δ T cells accumulate during wound healing and inflammation [8,9]. Mice lacking γ/δ T cell subset ($TCR\delta^{-/-}$) have enhanced bleomycin-induced lung fibrosis [10], and mice deficient in $V\gamma6/V\delta1^+$ T cells when treated with *Bacillus subtilis*

☆ This work was partially supported by Lydia O'Leary Memorial Foundation.
* Corresponding authors at: Department of Dermatology, Kanazawa University Graduate School of Medical Science, 13-1 Takaramachi, Kanazawa, Ishikawa 920-8641, Japan. Tel.: +81 76 265 2343; fax: +81 76 234 4270.
E-mail addresses: uedaik@hirakata.kmu.ac.jp (I. Ueda-Hayakawa), fujimoto-m@umin.ac.jp (M. Fujimoto).

0923-1811/$36.00
http://dx.doi.org/10.1016/j.jdermsci.2012.10.003